IQGAP1 Promotes Early B Cell Development, Is Essential for the Development of Marginal Zone (MZ) B Cells, and Is Critical for Both T-Dependent and T-Independent Antibody Responses

Ravi K Lella and Subramaniam Malarkannan *

Posted Date: 7 July 2023

doi: 10.20944/preprints202307.0442.v1

Keywords: B cell; development; IQGAP1; scaffold protein; signaling

Article

IQGAP1 Promotes Early B Cell Development, Is Essential for the Development of Marginal Zone (MZ) B Cells, and Is Critical for Both T-Dependent and T-Independent Antibody Responses

Ravi K Lella [1] and Subramaniam Malarkannan [1,2,3,4]

[1] Laboratory of Molecular Immunology and Immunotherapy, Blood Research Institute, Versiti, Milwaukee, WI; Departments of
[2] Microbiology and Immunology;
[3] Pediatrics,
[4] Medicine, and Medical College of Wisconsin, Milwaukee, WI
* Correspondence: should be addressed to S.M. (smalarkannan@versiti.org)

Abstract: IQGAP1 is a multi-functional scaffold protein. However, its role in B cell development and function is not known. Here, we demonstrate *Iqgap1*$^{-/-}$ mice contained significantly increased numbers of B220^{+} B, B220^{+}IgM^{-} pro/pre-B, and B220^{+}IgM^{+} immature-B cells in the bone marrow. Here, we show IQGAP1 as the essential scaffold that regulates early B cell development and function. *Iqgap1*$^{-/-}$ mice contained significantly increased numbers of B220^{+} B, B220^{+}IgM^{-} pro/pre-B, and B220^{+}IgM^{+} immature-B cells in the bone marrow. New-forming and follicular B cell numbers were increased, while the marginal zone B cell numbers were significantly reduced in the spleen of the *Iqgap1*$^{-/-}$ mice. Lack of IQGAP1 reduced T-dependent and T-independent humoral responses. Mechanistically, the lack of IQGAP1 considerably decreased the phosphorylation of Mek1/2, Erk1/2, and Jnk1/2. B cells from *Iqgap1*$^{-/-}$ mice failed to suppress IL-7R-mediated activation of Stat5a/b, an essential step for cell-cycle exit and initiate light-chain recombination, leading to a reduction in RS rearrangement frequency. Lack of IQGAP1 resulted in a significant reduction of IRF4 and IRF8 in BM B cells. Our study provides the first evidence that IQGAP1-based signalosome is essential for the development and functions of B cells.

Keywords: IQGAP1; B cell; MAPK; IQGAP1 signalosome

Introduction

The multi-functional scaffold IQGAP1 is a 190 kDa scaffold protein expressed in several cell types [1, 2, 3, 4, 5]. There are three members in the IQGAP family, conserved in humans and mice [6]. IQGAP1 is ubiquitously expressed [7], while IQGAP2 is found to be expressed in the liver, platelets, kidney, stomach, prostate, thyroid, and salivary glands [8, 9, 10, 11]. In contrast, the expression of IQGAP3 is different from the other two isoforms, primarily found in the brain, lung, testis, small intestine, and colon [8, 12]. Murine IQGAP1 and IQGAP2 isoforms share 52% of their amino acid identities with a 68% overall protein homology. IQGAP1 and IQGAP3 isoforms display 57% amino acid and 74% overall protein homology [13]. IQGAP1 possesses six well-defined interactive domains (**Figure 1A**), which interact with numerous cellular protein partners [14]. Among lymphocytes, murine NK, B, and T cells express IQGAP1[15, 16]. Earlier study has characterized the role of IQGAP1 in murine B cells in the context of Rap1-cofilin-1 pathway in actin reorganization and MTOC polarization[17]. However, its role in B cell development has not been explored.

Preprints (www.preprints.org) | NOT PEER-REVIEWED | Posted: 7 July 2023 doi:10.20944/preprints202307.0442.v1

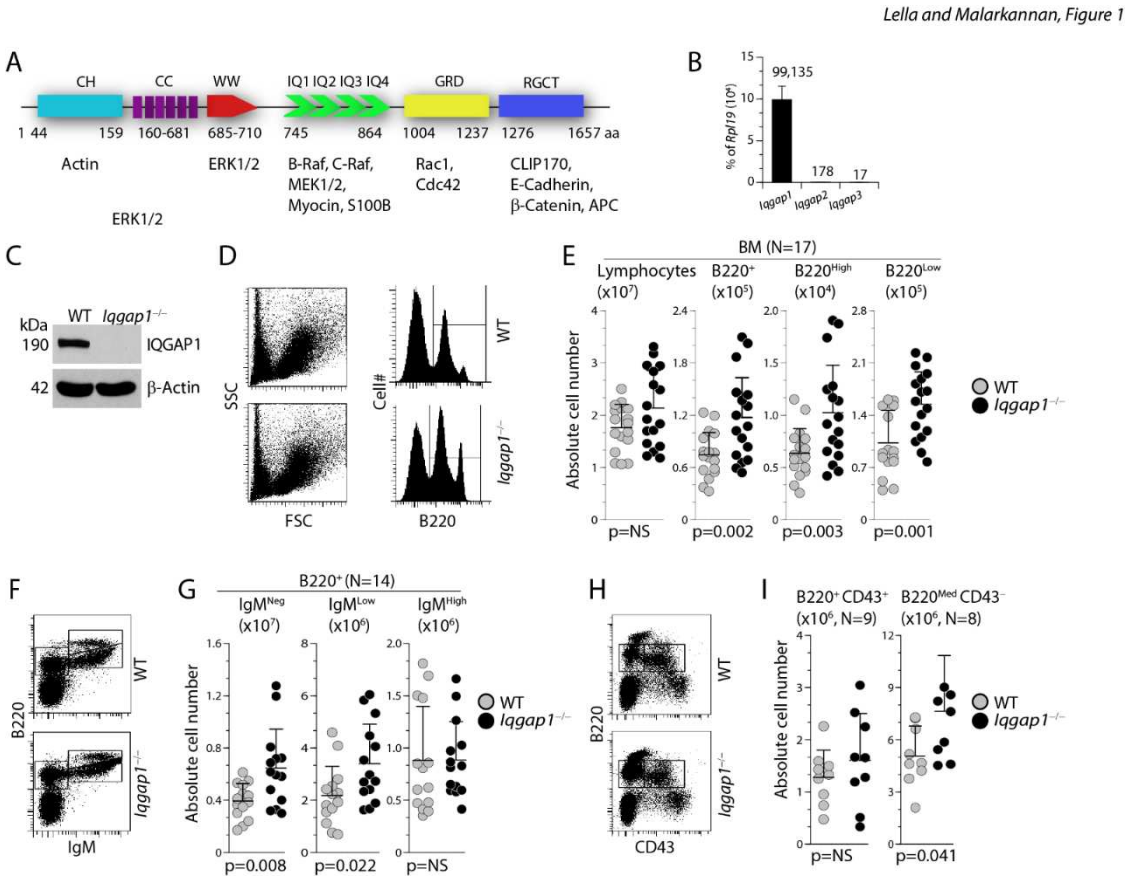

Figure 1. Lack of IQGAP1 results in dysregulated early B cell development in the BM. A) Calponin homology (CH) domain regulates the cytoskeleton by binding to N-WASp and F-actin. Coiled-coil (CC) regions, comprised of conserved amino acid repeats, bind to Ezrin. WW domain is involved in recruiting Erk1/2 to facilitate a sequential phosphorylation cascade. Isoleucine/glutamine-containing (IQ) domains recruit Rap1a, Rap1b, B-Raf, C-Raf, Mek1, and Mek2 to promote phosphoinositide (PIPKIγ) and calcium signaling. The Ras-GAP domain (GRD) interacts with small GTPases Cdc42, Rac1, and TC10. The Ras-GAP C-terminus (RGCT) domain interacts with CLIP-170, Clasp2, β-catenin, E-cadherin, and APC. **B**) Sorted total B220⁺ resting B cells from the BM were analyzed for the expression levels of *Iqgap1*, *Iqgap2*, and *Iqgap3* transcripts using RTqPCR. Relative expression of these transcripts is shown as percent of Rpl19 house-keeping gene. The data shown are the average of three independent experiments. **C**) Expression of IQGAP1 protein in the WT and *Iqgap1*$^{-/-}$ mice were analyzed by western blot using an anti-IQGAP1 antibody. Level of β-actin was used as loading controls. Blots are a representative set from three different experiments. **D, E**) Viable cells within the lymphocyte gate were analyzed for the absolute number of total B cells. Staining with anti-B220 antibody indicated the presence of both B220^{High} and B220^{Low} B cells in both the WT and *Iqgap1*$^{-/-}$ mice. **F, G**) Absolute numbers of B220^{+}IgM^{-} pro/pre-B, B220^{+}IgM^{+} immature B, and B220^{Hi} recirculating B cells were defined using anti-B220 and anti-IgM antibodies, and their numbers were calculated from live lymphocyte gates. **H, I**) The absolute numbers of pro-B cells were further identified with anti-B220 and anti-CD43 antibody staining. Pro-B cells are B220^{Med}CD43$^{+,}$ and pre-B cells are B220^{+}CD43^{-}. Data shown in C, E, and G are representative panels. Open and filled circles in D, F, and H are values obtained from an individual mouse from four independent experiments. Data are shown with the mean ± SEM. Statistical significance was calculated using Student's *t*-test, and p-values are shown below each graph.

Due to its ability to directly bind and cross-link F-actin, IQGAP1 plays an essential role in cytoskeletal maintenance and cell integrity, filopodia formation, and directional movement [18, 19]. Our earlier study identified an IQGAP1-based master signalosome upon receptor-mediated activation. This signalosome localized in the perinuclear region of murine NK cells coordinated the sequential

 doi:10.20944/preprints202307.0442.v1

phosphorylation of Raf→MEK1/2→ERK1/2 [15, 16]. The functional domains of IQGAP1 regulate several vital cellular processes, including actin/tubulin-mediated cytoskeletal remodeling, Erk1/2-mediated c-Fos, c-Jun, and Elk1 activation β-catenin-mediated LEF and TCF activation, and calmodulin-mediated Ca^{2+} signaling. Irrespective of these findings, the precise functions of IQGAP1 in B cells are yet to be determined.

Here, using wild-type (WT) and *Iqgap1*$^{-/-}$ mice, we found that lack of IQGAP1 significantly altered the development and function of different B cell subsets. The bone marrow (BM) of *Iqgap1*$^{-/-}$ mice contained significantly increased numbers of B220^{+} B, B220^{+}IgM^{-} pro/pre-B, and B220^{+}IgM^{+} immature-B cells. The new-forming (NF) and follicular (FO) B cell numbers were increased, while the marginal zone (MZ) B cell numbers were significantly reduced in the spleen of the *Iqgap1*$^{-/-}$ mice. These developmental defects are B cell-intrinsic, and the absence of IQGAP1 significantly reduced T-dependent (TD) and T-independent (TI) humoral responses. Mechanistically, lack of IQGAP1 resulted in the reduction of Mek1/2, Erk1/2, and Jnk1/2 phosphorylation following anti-IgM mAb-mediated activation. In addition, lack of IQGAP1 resulted in a substantial reduction in *Irf4* in both transcript and protein levels. B cells from *Iqgap1*$^{-/-}$ mice failed to suppress IL-7R-mediated activation of Stat5a and Stat5b, which resulted in a higher number of pro and pre-B cells. Analyses of recombining sequence (RS) rearrangement frequency demonstrate a moderate reduction in the absence of IQGAP1. Our study provides the first evidence that IQGAP1-based signalosome is essential for the development and functions of B cells.

Results

Iqgap1 is the dominant isoform in B cells

IQGAP1 possesses six functional domains (**Figure 1A**) and belongs to a three-member family. To determine the specific isoform expressed in B cells, we used non-overlapping primer sets to amplify and quantify the transcripts that encode *Iqgap1*, *Iqgap2*, and *Iqgap3* in bone marrow-derived total B cells. We found that only the transcripts expressing *Iqgap1* were the predominant isoform, and the *Iqgap2* and *Iqgap3* are undetectable in total B cells (**Figure 1B**). Therefore, to establish the role of IQGAP1 in B cell development and function, we used *Iqgap1* gene knockout mice (*Iqgap1*$^{-/-}$) [20]. Earlier genomic and biochemical studies confirmed that this insertion-deletion mutation targeting exons 26 and 27 of the *Iqgap1* gene resulted in a null allele [20]. Therefore, we analyzed the expression of the IQGAP1 protein in the wild-type (WT) and *Iqgap1*$^{-/-}$ mice. WT B cells contained a 190 kDa corresponding to the size of the full-length IQGAP1 protein, which was absent in *Iqgap1*$^{-/-}$ B cells (**Figure 1C**).

B cell development in the BM of Iqgap1$^{-/-}$ *mice is altered*

To investigate the role of IQGAP1 in B cell development, we analyzed the absolute numbers of B cells in the BM. The absolute numbers of total lymphocytes in the BM of *Iqgap1*$^{-/-}$ mice were comparable to that of WT (**Figure 1D, E**). Irrespective of this, the absolute numbers of B220^{+} B cells were significantly increased in the BM of *Iqgap1*$^{-/-}$ mice compared to that of WT (*Iqgap1*$^{-/-}$: 11.74 ± 4.72×10^{4}; WT: 7.46 ± 2.62×10^{4}; n=17, 17; and p=0.002) (**Figure 1D, E**). B220^{+} B cells can be further divided into B220^{High} and B220^{Low} subsets. *Iqgap1*$^{-/-}$ mice exhibited significant increases in both B220^{High} (*Iqgap1*$^{-/-}$: 10.2 ± 4.5×10^{5}; WT: 6.4 ± 2.3×10^{5}; n=17, 17; and p=0.003) and B220^{Low} subsets (*Iqgap1*$^{-/-}$: 1.55 ± 0.44×10^{4}; WT: 1.02 ± 0.43×10^{4}; n=17, 17; and p=0.001). Based on B220 and IgM expression, BM B cells are classified into pro/pre-B (B220^{+}IgM^{-}), immature B (B220^{+}IgM^{+}), and recirculating mature B cells (B220^{Hi}). The absolute numbers of B220^{+}IgM^{-} pro/pre (*Iqgap1*$^{-/-}$: 6.45 ± 3.0×10^{4}; WT: 3.94 ± 1.3×10^{4}; n=14, 14; and p=0.008) and recirculating mature B220^{+}IgM^{Low} population (*Iqgap1*$^{-/-}$: 3.4 ± 1.5×10^{4}; WT: 2.17 ± 1.11×10^{4}; n=14, 14; and p=0.022) were significantly increased in *Iqgap1*$^{-/-}$ mice compared to WT (**Figure 1F, G**). In contrast, the number of B220^{+}IgM^{+} immature B cells was comparable between *Iqgap1*$^{-/-}$ and WT mice (*Iqgap1*$^{-/-}$:0.89 ± 0.37×10^{4}; WT: 0.88 ± 0.52×10^{4}; n=14, 14; and p=NS) (**Figure 1G**). B cell development in BM can be further characterized through the expression of CD43 (Leukosialin), CD117 (c-Kit), and CD25 (IL-2Rα). Early Pro-B cells are

Preprints (www.preprints.org) | NOT PEER-REVIEWED | Posted: 7 July 2023 doi:10.20944/preprints202307.0442.v1

B220⁺CD43⁺, which develop into B220⁺CD43⁻ B cells. The absolute B220⁺CD43⁺ pro-B cell numbers did not differ significantly between *Iqgap1*$^{-/-}$ and WT (*Iqgap1*$^{-/-}$: 1.6 ± 0.89×10⁶ and WT: 1.3 ± 0.52×10⁶; n=9, 9; p=0.36) (**Figure 1H, I**).

Lack of IQGAP1 forms a blockade at early B cell development, and it is cell-autonomous

However, B220^{Med}CD43⁻ pre-B cells were significantly higher in *Iqgap1*$^{-/-}$ (*Iqgap1*$^{-/-}$: 7.6 ± 3.2×10⁶ and WT: 5.0 ± 1.7×10⁶; n=8, 8; p=0.041), which is consistent with the increased B220⁺IgM⁻ pro/pre-B cells populations. As pro-pre-B-I cells mature into pre-B-II (large and small), c-kit expression decreases and CD25 level increases. In this context, we also observed a significantly increased B220⁺CD25⁺ pre-B-II population (*Iqgap1*$^{-/-}$: 4.10 ± 2.16×10⁶ and WT: 2.35 ± 1.31×10⁴; n=9, 9; p=0.05) in *Iqgap1*$^{-/-}$ mice (**Figure 2A, B**). BM-derived cells were also stained with anti-B220, anti-IgM, and anti-IgD Abs and analyzed. The absolute numbers of IgM⁺IgD⁺ (*Iqgap1*$^{-/-}$: 0.57 ± 0.25×10⁴and WT: 0.42 ± 0.19×10⁴; n=13, 13; p=NS) and IgM⁻IgD⁺ (*Iqgap1*$^{-/-}$: 0.48 ± 0.15×10⁴ and WT: 0.52 ± 0.25×10⁴; n=13, 13; p=NS) B cells were comparable between *Iqgap1*$^{-/-}$ and WT mice (**Figure 2C, D**). However, both the immature IgM⁻IgD⁻ (*Iqgap1*$^{-/-}$: 6.8 ± 3.0×10⁴ and WT: 4.0 ± 1.3×10⁴; n=13, 13; p=0.008) and IgM⁺IgD⁻ (*Iqgap1*$^{-/-}$: 3.38 ± 1.68×10⁴ and WT: 1.71 ± 0.62×10⁴; n=13, 13; p=0.003) B cells were increased in *Iqgap1*$^{-/-}$ mice compared to that of WT (**Figure 2C, D**), indicating a loss of developmental regulation during the early stages of B cell maturation.

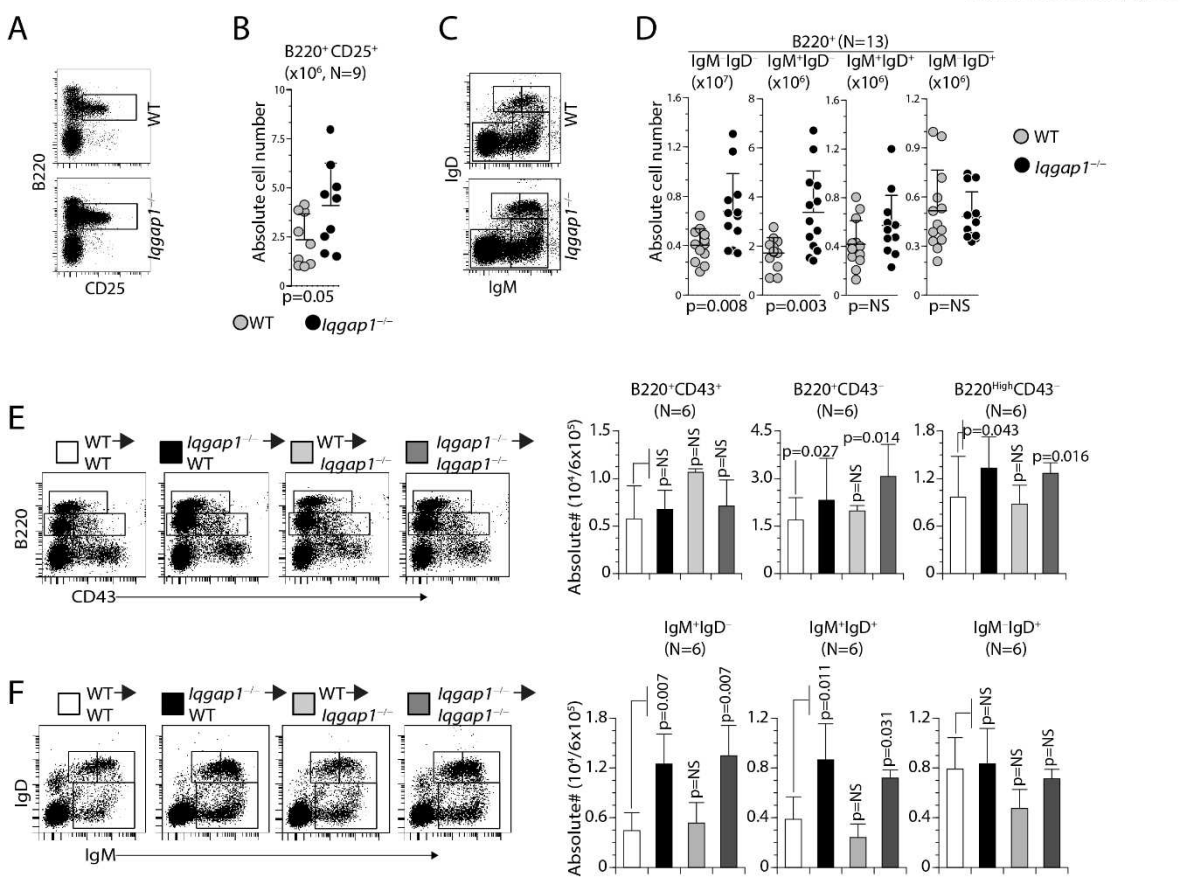

Figure 2. Lack of IQGAP1 leads to a potential blockade at pre-B cell stages in the BM and the defects in the transition of pro-B to pre-B cells in the BM of *Iqgap1*$^{-/-}$ mice is cell-intrinsic. A, B) Absolute numbers of B220⁺CD25⁺ large and small pre-B-II stage. C, D) Absolute numbers of B220⁺IgM⁻IgD⁻ or B220⁺IgM⁺IgD⁻ immature B and B220⁺IgM⁺IgD⁺ or B220⁺IgM⁻IgD⁺ mature B cells. BM cells were stained with anti-B220, anti-IgM, and anti-IgD antibodies, and the absolute numbers were calculated per million total gated lymphocytes. Data shown in A, C, and E are one representative panel from a minimum of three independent experiments. Open and filled circles in B and D are values obtained from an individual mouse from four independent experiments. Data are shown with the mean ± SEM. Statistical significance was calculated using Student's *t*-test, and p-values are shown

Preprints (www.preprints.org) | NOT PEER-REVIEWED | Posted: 7 July 2023 doi:10.20944/preprints202307.0442.v1

below each graph. E) Indicated host mice were sub-lethally irradiated and reconstituted with donor-derived 5 × 10^5 BM cells. Eight weeks later, cells from the host BM were harvested and analyzed. The absolute numbers of reconstituted pro-B cells were identified with anti-B220 and anti-CD43 antibody staining. Pro-B cells ($B220^{Med}CD43^+$) and pre-B cells ($B220^+CD43^-$) were quantified from six host mice, and the average absolute numbers are presented as bar graphs. F) Absolute numbers of reconstituted $B220^+IgM^-IgD^-$ or $B220^+IgM^+IgD^-$ immature B and $B220^+IgM^+IgD^+$ or $B220^+IgM^-IgD^+$ mature B cells. BM cells were stained with anti-B220, anti-IgM, and anti-IgD antibodies, and the absolute numbers were calculated per million total gated lymphocytes. Data shown on the left are representative panels. The average absolute numbers are presented as bar graphs. Data shown are from two independent experiments with three mice each. Data are shown with the mean ± SEM. Statistical significance was calculated using Student's *t*-test, and p-values are shown below each graph.

IQGAP1 is expressed in most of the hematopoietic cell lineages [21]. Since IQGAP1 has been globally deleted [20] in the mice we used, the defects we observed in absolute B cell numbers can be cell-intrinsic or due to an abnormality in the stromal microenvironment. To distinguish between these two possibilities, we performed bone marrow (BM) transplantation (WT→WT; *Iqgap1*$^{-/-}$→WT; WT→*Iqgap1*$^{-/-}$; *Iqgap1*$^{-/-}$→*Iqgap1*$^{-/-}$). After eight weeks, B cell development was analyzed in the reconstituted host mice. Lymphocyte reconstitution was successfully observed in all hosts. Compared to WT, the transfer of *Iqgap1*$^{-/-}$ BM cells into WT or *Iqgap1*$^{-/-}$ hosts resulted in an increased absolute number of lymphocytes in the BM (**Supplementary Figure S1A**). Absolute numbers of $B220^+$ B, $B220^{High}$, and $B220^{Low}$ cell numbers were significantly increased in host mice that received *IQGAP1*$^{-/-}$ BM cells (**Supplementary Figure S1B**). Also, although $B220^+IgM^{Neg}$ cells did not show any considerable change, $B220^+IgM^{High}$ and $B220^+IgM^{Low}$ cells were significantly increased in the recipient mice that were transplanted with *Iqgap1*$^{-/-}$ BM cells compared to that of WT (**Supplementary Figure S1C**). Analyzing Pro/Pre-B cells ($B220^+CD43^+$), Pro-B cells ($B220^{Med}CD43^-$), and Pre-B cells ($B220^{High}CD43^-$) in reconstituted mice confirmed accumulation of Pro-B cells (**Figure 2E**). Staining for immature (IgM^+IgD^-) and mature (IgM^+IgD^+ and IgM^-IgD^+) B cell populations in the reconstituted mice indicated a significant increase in the immature but not the mature B cells (**Figure 2F**). In the spleens from the BM reconstituted mice, we did not observe an increase in the absolute number of lymphocytes or $B220^+$ B cells (**Supplementary Figure S2A**). However, the transfer of *Iqgap1*$^{-/-}$ BM cells into the WT or *Iqgap1*$^{-/-}$ mice lead to a significant increase in the absolute numbers of immature (IgM^+IgD^-) but not mature (IgM^+IgD^+ and IgM^-IgD^+) B cell populations (**Supplementary Figure S2B**). These results demonstrate that the lack of IQGAP1 in the hematopoietic compartment but not the stromal environment is primarily responsible for the B cell developmental defects.

Lack of IQGAP1 significantly increases $IgM^{High}CD23^-$ T1 B cells in the spleens

Next, we analyzed the B cell maturation in the spleen. Lack of IQGAP1 did not alter the total lymphocyte numbers in the *Iqgap1*$^{-/-}$ mice (*Iqgap1*$^{-/-}$: 39.0 ± 8.2×10^6 and WT: 40.1 ± 8.4×10^6; n=16, 16; p=NS) (**Figure 3A**). Moreover, similar to the BM, the absolute numbers of $B220^+$ B cells in the spleen were moderately but significantly increased in *Iqgap1*$^{-/-}$ compared to that of the WT mice (*Iqgap1*$^{-/-}$: 16.58 ± 6.26×10^6 and WT: 13.17 ± 5.16×10^6; n=31, 31; p=0.022) (**Figure 3B**). To further analyze the role of IQGAP1 in splenic B cell development, we stained them with anti-IgM and anti-IgD Abs. Although there were moderate increases in immature IgM^+IgD^- B (*Iqgap1*$^{-/-}$: 2.91 ± 2.17×10^6 and WT: 1.85 ± 1.37×10^6; n=12, 12; p=NS) and mature IgM^+IgD^+ (*Iqgap1*$^{-/-}$: 5.3 ± 2. 95×10^6 and WT: 3.46 ± 2.01×10^6; n=12, 12; p=NS) or IgM^-IgD^+ (*Iqgap1*$^{-/-}$: 5.08 ± 2.49×10^6 and WT: 3.88 ± 1.82×10^6; n=12, 12; p=NS) B cells in the spleen of *Iqgap1*$^{-/-}$ mice, they did not differ significantly (**Figure 3C**).

Preprints (www.preprints.org) | NOT PEER-REVIEWED | Posted: 7 July 2023 doi:10.20944/preprints202307.0442.v1

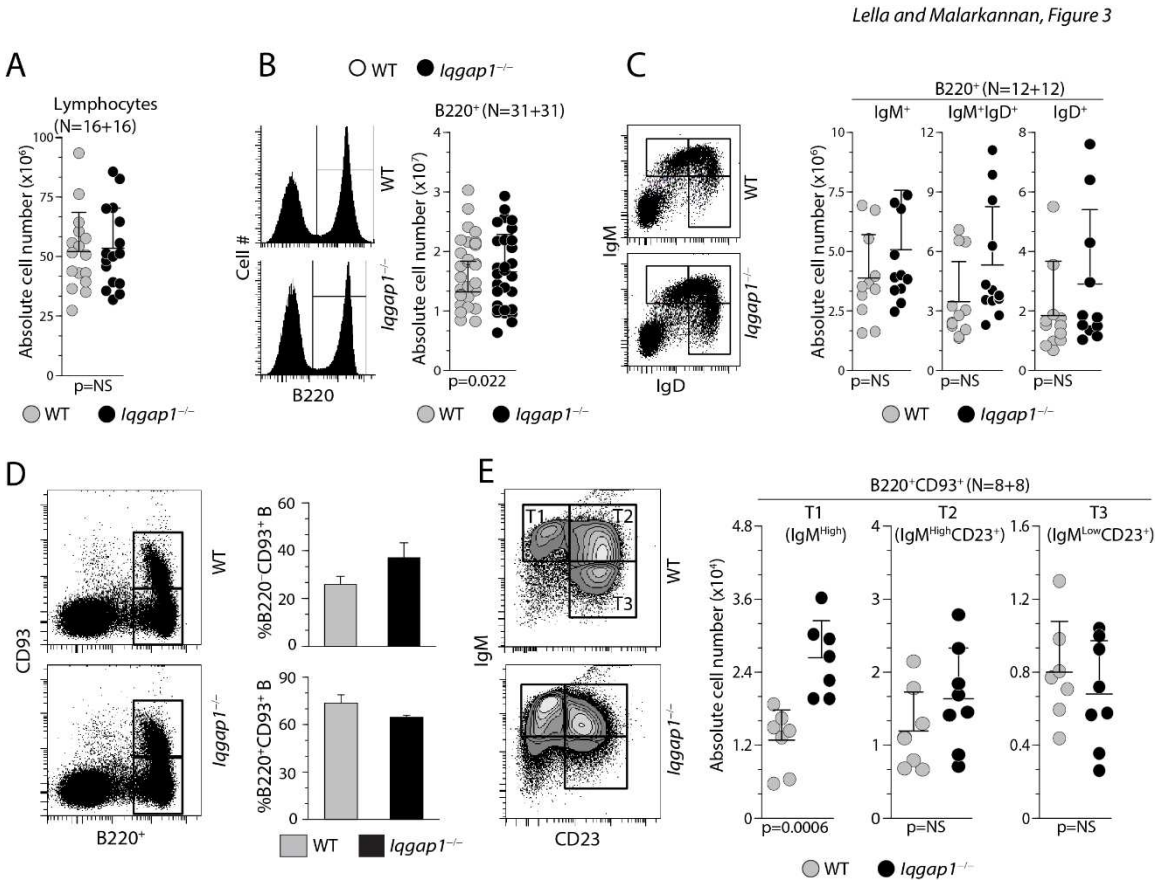

Figure 3. Lack of IQGAP1 leads to increased T1 B cells in the spleen. A) Absolute number of total lymphocytes within the spleens of WT and *Iqgap1*$^{-/-}$ mice were comparable. Absolute numbers were calculated from live gating of the lymphocyte population. Data shown represent the total lymphocytes per spleen from both strains. **B**) Absolute total splenic B cells were comparable between the WT and *Iqgap1*$^{-/-}$ mice. Viable cells within the lymphocyte gate were analyzed for the absolute number of total B cells using anti-B220 antibody. Data shown represent the B220^{+} B cells per spleen from both strains. **C**) Absolute numbers of immature and mature B cells do not differ between the WT and *Iqgap1*$^{-/-}$ mice. Total splenic B cells were stained with anti-B220, anti-IgM, and anti-IgD antibodies. Data shown represent the B220^{+}IgM^{+} immature B and B220^{+}IgM^{+}IgD^{+} or B220^{+}IgM^{-}IgD^{+} mature B cells. Data represent absolute numbers of immature or mature B cells per spleen from both strains. **D**) Absolute numbers of T1-B but not T2-B or T3-B are altered in *Iqgap1*$^{-/-}$ mice. Total splenocytes were stained with anti-B220, and anti-CD93 antibodies and the double-positive cells were gated and quantified. **E**) B220^{+}CD93^{+} B cells were further sub-divided into B220^{+}CD93^{+}IgM^{+} T1-B, B220^{+}CD93^{+}IgM^{+}CD23^{+} T2-B, and B220^{+}CD93^{+}IgM^{-}CD24^{+} T3-B cells. Open and filled circles in A, B, C, and E are values obtained from an individual mouse from four independent experiments. Data are shown with the mean ± SEM. Statistical significance was calculated using Student's *t*-test, and p-values are shown below each graph.

Next, we identified the transitional B cells among the total B220^{+} splenocytes based on their CD93 positivity. Transitional T1, T2, and T3 B cells are defined as IgM^{High}CD23^{-}, IgM^{High}CD23^{+}, and IgM^{Low}CD23^{+}, respectively. We gated the B220^{+} splenocytes into CD93^{+} and CD93^{-} B cells (**Figure 3D**). We selected the CD93^{+} B cells and subdivided them based on IgM and CD23 positivity. Total percentages of B220^{+}CD93^{+} B cells did not vary between the WT and the *Iqgap1*$^{-/-}$ splenocytes. However, the absolute number of IgM^{High}CD23^{-} T1 B cells was significantly increased among the splenocytes from *Iqgap1*$^{-/-}$ mice (**Figure 3E**). Absolute numbers of T2 and T3 B cells were comparable between the WT and the *Iqgap1*$^{-/-}$ mice.

Preprints (www.preprints.org) | NOT PEER-REVIEWED | Posted: 7 July 2023 doi:10.20944/preprints202307.0442.v1

Lack of IQGAP1 differentially affects FO B and MZ B cells in the spleens

B220⁺ splenic B cells can also be separated into new-forming (NF B) ($CD21^{Low/-}CD23^{Low/-}$), follicular (FO B) ($CD23^{High}CD21^{Low/-}$) and marginal zone (MZ B) ($CD21^{High}CD23^{Low/-}$) cells. Therefore, we next analyzed the numbers FO, NF, and MZ B cells (**Figure 4A**). The absolute numbers of B220-gated $CD21^{Low/-}CD23^{High}$ FO B (*Iqgap1*$^{-/-}$: 11.7 ± 3.5×10⁶ and WT: 8.92 ± 3.82×10⁶; n=14, 14; p=0.026) and the $CD21^{Low/-}CD23^{Low/-}$ NF B cells (*Iqgap1*$^{-/-}$: 6.37 ± 2.71×10⁶ and WT: 4.33 ± 1.18×10⁶; n=14, 14; p=0.018) were significantly increased in *Iqgap1*$^{-/-}$ mice. However, the absolute number of MZ B was significantly reduced in the spleens of *IQGAP1*$^{-/-}$ mice (*Iqgap1*$^{-/-}$: 1.18 ± 0.6×10⁶ and WT: 1.59 ± 0.87×10⁶; n=14, 14; p=0.05). In addition to these changes, the B cell follicles in the spleens of *Iqgap1*$^{-/-}$ mice were extended and multi-centered compared to that of WT**.** MZ B cells can also be defined by their exclusive high-level expression of IgM, CD21, and CD1d [22]. Staining for IgM and CD21 (*Iqgap1*$^{-/-}$: 0.93 ± 0.44×10⁶ and WT: 1.56 ± 0.0.53×10⁶; n=11, 11; p=0.0049) or IgM and CD1d (*Iqgap1*$^{-/-}$: 0.75 ± 0.32×10⁶ and WT: 1.18 ± 0.31×10⁶; n=9, 9; p=0.0364) confirmed the significant decrease in the absolute number of MZ B cells (**Figure 4B, C)**. We immune-stained spleen cryosections to establish further the exclusive reduction in MZ B cells. *Iqgap1*$^{-/-}$ mice displayed normal B cell follicle architecture (**Figure 4D**), as revealed by the anti-CD3ε and anti-B220 mAb staining. Since the metallophilic macrophages form a boundary between the follicular and marginal zones, we used MOMA-1 mAb to determine the changes in the marginal zone. The spleen sections from the WT mice revealed a well-defined band of B220⁺ MZ area outside of the MOMA-1⁺ metallophilic macrophages. However, similar regions were greatly reduced and less contiguous in *Iqgap1*$^{-/-}$ mice, which further confirmed a reduction in the number of MZ B cells (**Figure 4E**).

Lella and Malarkannan, Figure 4

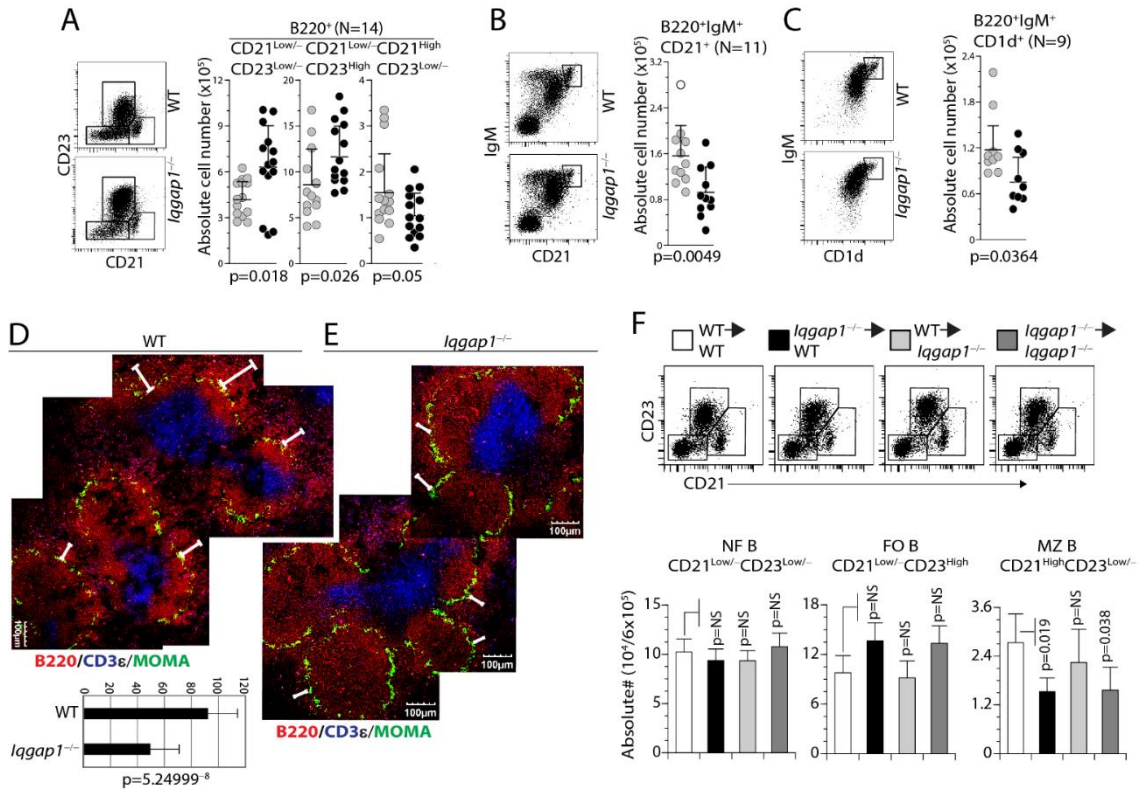

Figure 4. Lack of IQGAP1 leads to increased NF-B, FO-B but decreased MZ-B cells in the spleen and the dysregulated early B cell development in the spleen of *Iqgap1*$^{-/-}$ mice is B cell-intrinsic. A) Absolute numbers of $CD21^{Low/-}CD23^{Low/-}$ NF-B, $CD21^{Low}CD23^{High}$ FO-B, and $CD21^{High}CD23^{Low/-}$ MZ-B cells are shown. Total splenic B cells were stained with anti-B220, anti-CD21, and anti-CD23 antibodies, and live cells were gated and compared between the WT and *Iqgap1*$^{-/-}$ mice. Data shown represent absolute numbers per million live B220⁺ B cells. B) Reduction in MZ-B cells was validated using anti-IgM and anti-CD21 antibody staining of total B220⁺ splenic B cells. Data shown represent absolute

Preprints (www.preprints.org) | NOT PEER-REVIEWED | Posted: 7 July 2023 doi:10.20944/preprints202307.0442.v1

numbers per million live B220$^+$ B cells. C) Reduction in MZ-B cells was validated using anti-IgM and anti-CD1d antibody staining of total B220$^+$ splenic B cells. Data shown represent absolute numbers per million live B220$^+$ B cells. Open and filled circles in A, B, and C are values obtained from an individual mouse from four independent experiments. Data are shown with the mean ± SEM. Statistical significance was calculated using Student's *t*-test, and p-values are shown below each graph. D, E) Immunohistochemical analyses of splenic sections from WT and *Iqgap1*$^{-/-}$ mice. Spleens were isolated, embedded in paraffin, 7-micron thick sections were cut, and stained for total B cells (anti-B220), T cells (anti-CD3ε), and metallophilic macrophages (anti-MOMA antibody). Panels show the locations of T and B cells as part of the B cell follicles and metalophillic antigen-1$^+$ macrophages surrounding the follicles. F) Indicated host mice were sub-lethally irradiated and reconstituted with donor-derived 5 × 10^5 BM cells. Eight weeks later, cells from the host BM were harvested and analyzed. Absolute numbers of reconstituted CD21$^{Low/-}$CD23$^{Low/-}$ NF-B, CD21^{Low}CD23^{High} FO-B, and CD21^{High}CD23$^{Low/-}$ MZ-B cells are shown. Total splenic B cells were stained with anti-B220, anti-CD21, and anti-CD23 antibodies, and live cells were gated and compared between the WT and *Iqgap1*$^{-/-}$ mice. Data shown represent absolute numbers per million live B220$^+$ B cells.

These reductions were B cell-intrinsic as reconstitution with *Iqgap1*$^{-/-}$ BM cells either into WT or *Iqgap1*$^{-/-}$ mice confirmed these defects. In the spleen of the reconstituted mice, we did not observe an increase in the absolute number of lymphocytes or B220$^+$ B cells. However, the transfer of *Iqgap1*$^{-/-}$ BM cells into the WT or *Iqgap1*$^{-/-}$ mice lead to a significant increase in the absolute numbers of immature (IgM$^+$IgD$^-$) but not mature (IgM$^+$IgD$^+$ and IgM$^-$IgD$^+$) B cell populations. Reconstitution with *Iqgap1*$^{-/-}$ BM cells either into WT or *Iqgap1*$^{-/-}$ mice showed an increase in the CD23^{Hi}CD21$^{Low/-}$ FO B and a decrease in CD21^{Hi}CD23$^{Low/-}$ MZ B cells (**Figure 4F**). A decrease in the MZ B cells was further validated by a reduction in IgM$^+$CD21^{High} or IgM$^+$CD1d^{High} B cells in the reconstituted mice (**Figure 5A, B**). Our results demonstrate that the B cell defects in the BM and spleen of *Iqgap1*$^{-/-}$ mice were cell-intrinsic.

Lella and Malarkannan, Figure 5

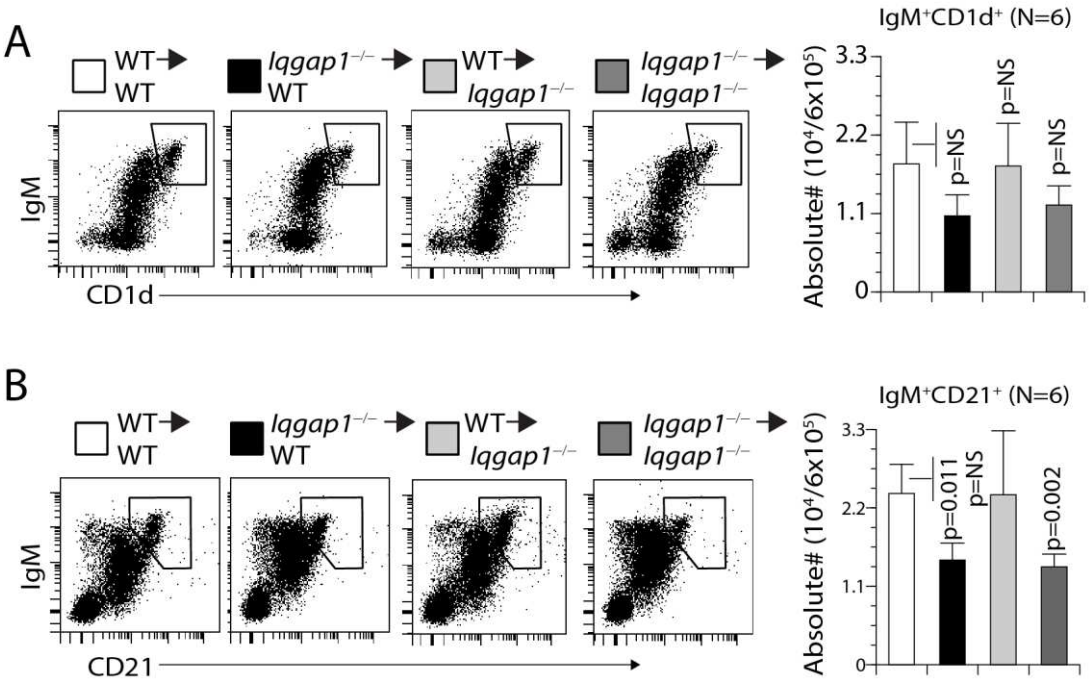

Figure 5. Dysregulated early B cell development in the spleen of *Iqgap1*$^{-/-}$ mice is B cell-intrinsic. **A**) Reduction in reconstituted MZ-B cells was validated using anti-IgM and anti-CD1d antibody staining of total B220$^+$ splenic B cells. Data shown represent absolute numbers per million live B220$^+$ B cells. **B**) Reduction in reconstituted MZ-B cells was validated using anti-IgM and anti-CD21antibody staining of total B220$^+$ splenic B cells. Data shown represent absolute numbers per million live B220$^+$

 doi:10.20944/preprints202307.0442.v1

B cells. Data are shown with the mean ± SEM. Statistical significance was calculated using Student's *t*-test, and p-values are shown below each graph.

Lack of IQGAP1 impairs T-independent and T-dependent antibody production

The significant impairment in B cell response in *Iqgap1*$^{-/-}$ mice could be due to either a developmental or a functional defect. To narrow it down, we first analyzed the basal immunoglobulin levels in the pre-immune sera of WT and *Iqgap1*$^{-/-}$ mice. Then, we quantified each isotype in the pre-immune sera. **Figure 6A** shows that IgG1, IgG2a, IgG2b, and IgA levels were comparable between WT and *Iqgap1*$^{-/-}$ mice. However, the levels of IgM were significantly reduced, and IgG3 was significantly increased in the sera of *Iqgap1*$^{-/-}$ mice (**Figure 6A**). Secreted 'natural' IgM is central to neutralizing pathogens and self-antigens. Thus, the presence of multiple Ig isotypes in the sera of *Iqgap1*$^{-/-}$ mice indicated that the lack of IQGAP1 did not result in a global hypo-responsiveness of B cells. IgG3 subtype possesses an extended hinge region, superior molecular flexibility, broad polymorphisms, and unique glycosylation sites compared to other IgG subclasses.

Preprints (www.preprints.org) | NOT PEER-REVIEWED | Posted: 7 July 2023 doi:10.20944/preprints202307.0442.v1

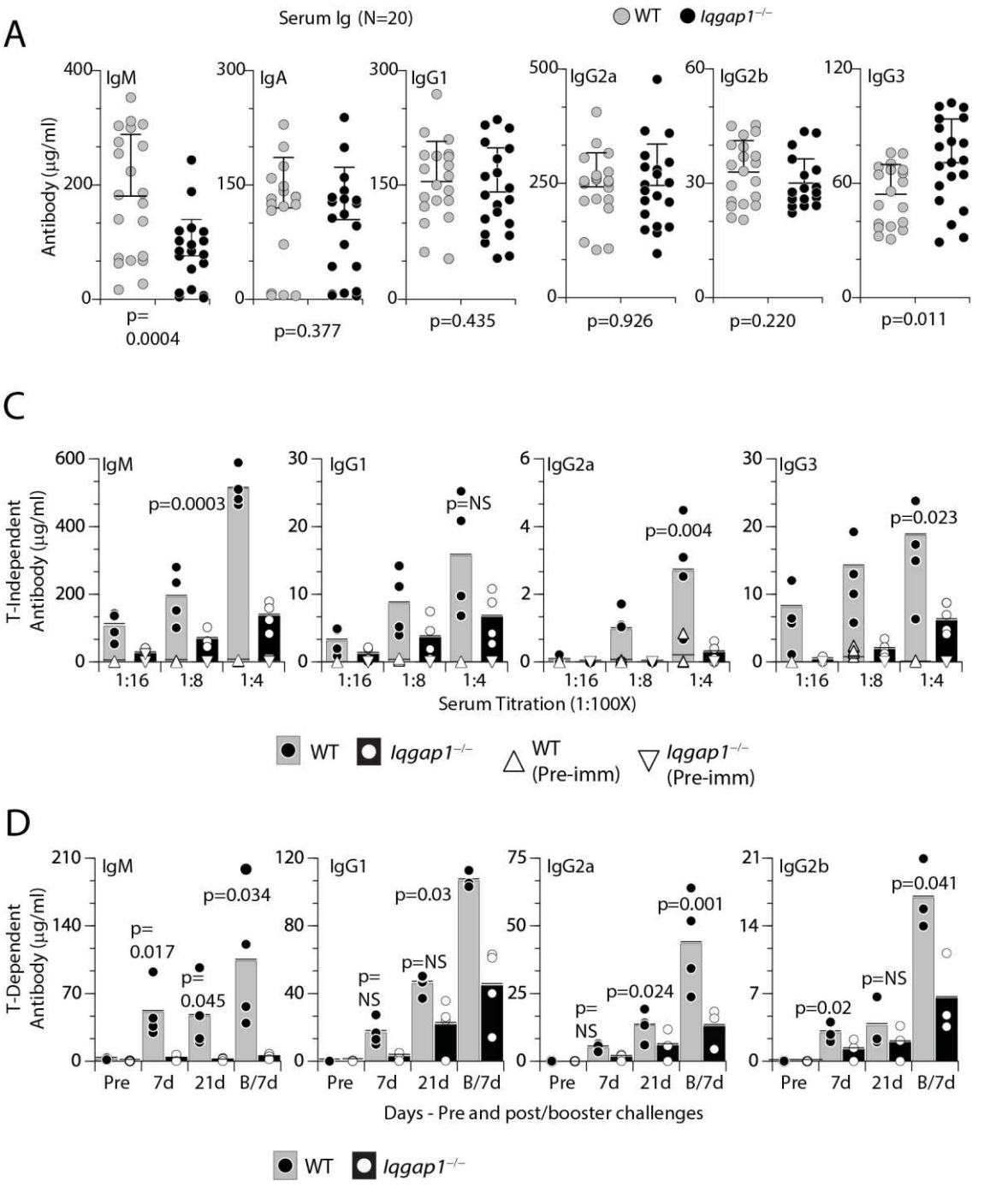

Figure 6. Lack of IQGAP1 results in significantly reduced IgM and IgG3 levels in the sera of *Iqgap1*$^{-/-}$ mice and results in significantly reduced T-independent and T-dependent humoral responses. A) Pre-immune sera were collected from 20 WT or *Iqgap1*$^{-/-}$ mice each and were analyzed for the levels of soluble IgM, IgA, IgG1, IgG2a, IgG2b, and IgG3 using isotype-specific capture and detection antibodies-based ELISA. Data presented were an average of duplicates for each isotype of each serum from multiple experiments. A total of 20 sera were used for each strain. Data are shown with the mean ± SEM. Statistical significance was calculated using Student's *t*-test, and p-values are shown below each graph. B) T-independent B cell responses were measured following the TNP-AECM-Ficoll antigen challenge. Four WT or four *Iqgap1*$^{-/-}$ mice were used to collect pre-immune or immune sera. ELISA was performed with titrated concentrations of sera (1:4, 1:8, and 1:16). IgM, IgG1, IgG2a, and IgG3 isotypes were tested and shown. C) T-dependent B cell responses were measured

Preprints (www.preprints.org) | NOT PEER-REVIEWED | Posted: 7 July 2023 doi:10.20944/preprints202307.0442.v1

following the TNP-KLH antigen challenge. Four WT or four *Iqgap1*$^{-/-}$ mice were used to collect pre-immune or immune sera. ELISA was performed with sera collected at different time points before (pre-immune) and after antigen challenge (post 7d, 21d, and following 7d after booster challenge). IgM, IgG1, IgG2a, and IgG2b isotypes were tested and shown. Open and filled circles in A and B are values obtained from an individual mouse. Black and grey bars represent, respectively. Statistical significance was calculated using Student's *t*-test, and p-values are shown below each graph.

To test whether IQGAP1 plays a role in humoral immune responses, we challenged age and sex-matched WT and *Iqgap1*$^{-/-}$ mice with T-independent (TI) antigen TNP-AECM-Ficoll (*TNP* (2,4,6-Trinitrophenyl), where the hapten is conjugated to Amino Ethyl Carboxy Methyl-Ficoll and collected sera to analyze the presence of antigen-specific IgM, IgG1, IgG2a, or IgG3. Our phenotypic analyses indicated an increased number of naïve B cells in *Iqgap1*$^{-/-}$ mice expressed membrane-bound IgM and IgD in both the BM and spleen. Irrespective of this and an increase in the overall FO B cell number, *Iqgap1*$^{-/-}$ mice could not produce similar amounts of TNP-specific antibodies during TI responses as WT mice (**Figure 6B**). Next, we examined the T-dependent (TD) immune responses by intraperitoneal injection of TNP-KLH. In the primary response, the generation of TNP-specific IgM, IgG1, IgG2a, or IgG2b was significantly reduced in *Iqgap1*$^{-/-}$ mice when compared to that of WT mice (**Figure 6C**). Further, after the antigen boost, the KLH-specific IgG1 did not recover and remained significantly low in the *Iqgap1*$^{-/-}$ mice compared to WT (**Figure 6C**). These results demonstrate that IQGAP1 plays a crucial role in the activation and functions of B cells.

Receptor editing at κ the locus is moderately defective in B cells lacking IQGAP1

The diversity in the length of hypervariable complementarity-determining region 3 (CDR3) of the heavy chain (CDRH3) indicates a repertoire of rearranged V_H genes and polyclonality [23]. Using PCR-based spectrotyping, we analyzed the fragment size and peak height for IgHV3, IgHV5, IgHV6, and IgHV7 in B cells from the BM. Our results show that the length of the variable regions and the relative number of sequence-occurrences of the heavy chains in B cells from the WT and *Iqgap1*$^{-/-}$ mice followed an expected normal Gaussian distribution indicative of diverse and comparable repertoire (**Figure 7A**). Thus, the lack of IQGAP1 did not affect the B cell repertoire diversity at the heavy chain rearrangement. Furthermore, the preserved heavy chain rearrangement in B cells from *Iqgap1*$^{-/-}$ mice indicated that lack of IQGAP1 did not affect the B cell repertoire diversity at the heavy chain rearrangement.

Preprints (www.preprints.org) | NOT PEER-REVIEWED | Posted: 7 July 2023 doi:10.20944/preprints202307.0442.v1

Lella and Malarkannan, Figure 7

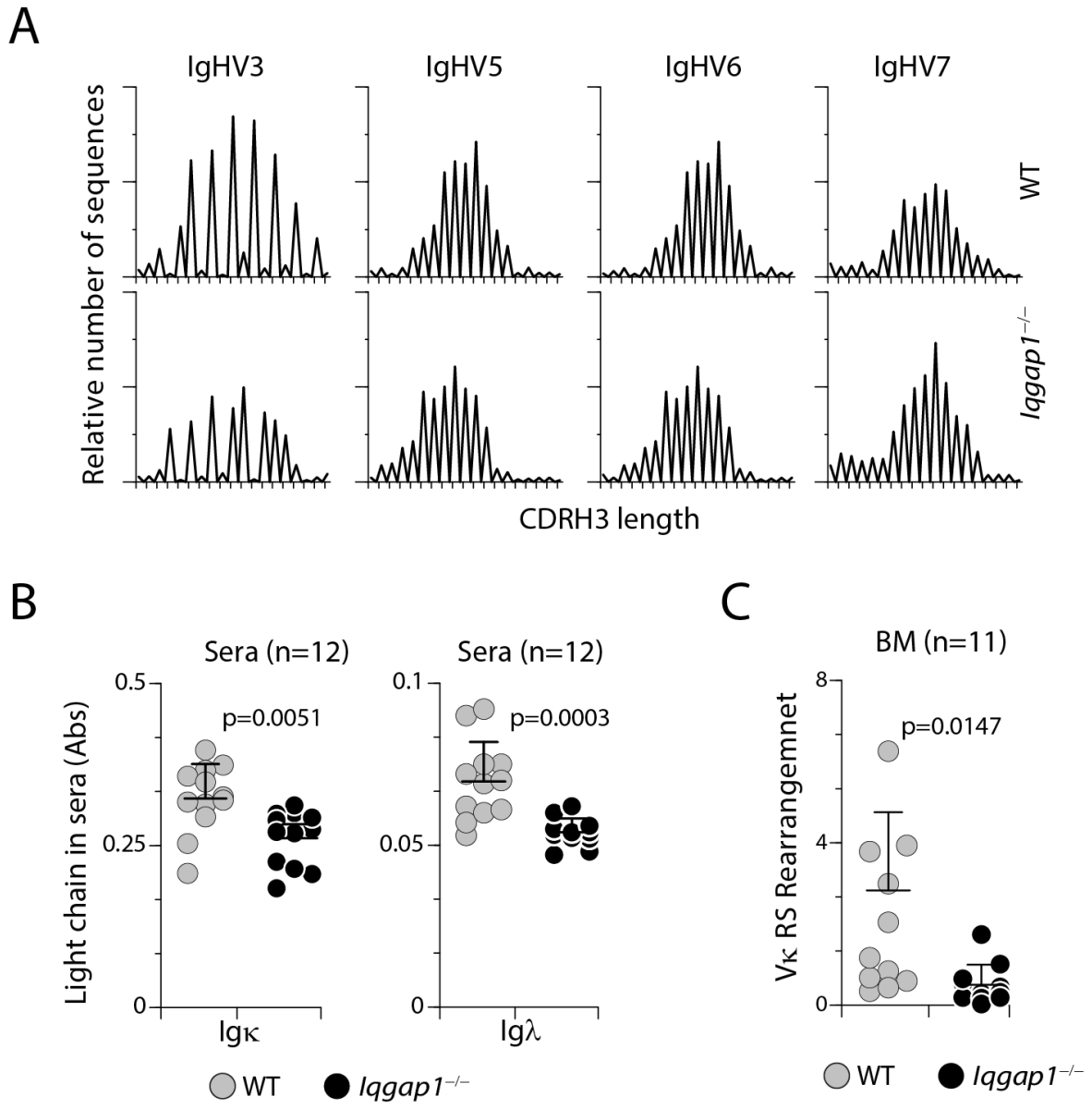

Figure 7. Light chain but not heavy recombination is affected by the lack of IQGAP1. A) PCR-based spectrotyping was employed to quantify the diversity in the length of hypervariable CDR3 of the heavy chain (CDRH3) in B cells from the BM of WT and *Iqgap1*$^{-/-}$ mice. The fragment size and peak height for IgHV3, IgHV5, IgHV6, and IgHV7 indicated that the repertoire of rearrangement V_H genes and polyclonality between these two strains are comparable and followed the expected normal Gaussian distribution indicative of diverse and comparable repertoire. **B**) Igκ and Igλ light chains in the sera are reduced in *Iqgap1*$^{-/-}$ mice. **C**) RS rearrangement at the k-locus is reduced in the absence of IQGAP1. Statistical significance was calculated using Student's *t*-test, and p-values are shown below each graph.

CD43^{+} B cell progenitors in mice rearrange immunoglobulin Igκ genes before the assembly of a productive $V_HD_HJ_H$ joint. Thus, μ chain rearrangement and expression are not prerequisites to Igκ light chain gene rearrangements in normal development [24]. Therefore, we next analyzed the quantity of κ and λ light chains in the sera of non-challenged healthy WT and *Iqgap1*$^{-/-}$ mice using an ELISA-based assay. We found a significant reduction in both the κ and λ light chains in *Iqgap1*$^{-/-}$ mice compared to the WT (**Figure 7B**). This demonstrates that the defect we see in the antibody production

Preprints (www.preprints.org) | NOT PEER-REVIEWED | Posted: 7 July 2023 doi:10.20944/preprints202307.0442.v1

in challenged mice could be related to the production of the light but not the heavy chains. Indeed small GTPase, Ras, plays an essential role via Mek1/2 and Erk1/2 in silencing *Ccnd3* transcription, exiting from the cell cycle, and initiating Igκ recombination and light chain editing [25]. Receptor editing in the light chain loci forms a critical basis for high-affinity maturation that is a continuous process in an ongoing immune response [26, 27], and impairment in κ chain rearrangement could account for the functional defects in T-dependent and independent antibody responses. Therefore, we next analyzed the light chain rearrangement. The orderly recombination of genes at the κ locus is the first step in the light chain rearrangement. The successful recombination of genes at the κ locus is proceeded by rearranging non-coding gene segments defined as 'recombining sequence' (RS) [28]. RS rearrangements occur higher in the most highly edited B cells. Thus, quantifying RS provides a readout for successful κ chain rearrangement [29]. Our results show that the levels of amplified RS products were moderately lower in the B cells derived from *Iqgap1*$^{-/-}$ mice (**Figure 7C**), indicating that the early pre-B cell development is largely intact in *Iqgap1*$^{-/-}$ mice. Thus, the functional defects observed in the B cells from *Iqgap1*$^{-/-}$ mice are due to an inability to rearrange the light chains appropriately.

B cell activation requires IQGAP1-Mek1/2-Erk1/2 signalosome

IQGAP1 is an essential scaffold in organizing Erk1/2 activation and phosphorylation [30]. Four tandem Isoleucine-Glutamine (IQ) domains are located between 745-864 amino acids. These IQ domains primarily mediate interactions with Rap1 [31], B-Raf or C-Raf [32], and Mek1/2 [30]. Therefore, we hypothesized that IQGAP1 regulates the sequential activation of the Raf/Mek1/2/Erk1/2 cascade. To test this, we activated purified total splenic B cells with soluble anti-IgM mAb. Rac1/Cdc42 activates p21-activated kinase (Pak) that connects the upstream signaling to Raf by phosphorylating S445 in B-Raf and S338 in C-Raf [33]. We found comparable amounts of phosphorylated B-Raf (Serine 445), C-Raf (Serine 338), and total B-Raf and C-Raf were present in *Iqgap1*$^{-/-}$ and WT B cells (**Figure 8A**). B-Raf or C-Raf catalyzes the phosphorylation of Mek1/2, which in turn phosphorylates Erk1/2 [34]. Since IQ domains recruit Mek1/2, we analyzed their activation status. and found the phosphorylation of Mek1/2 were considerably reduced in B cells lacking IQGAP1. The WW domain of IQGAP1 (685-710 amino acids) contains two conserved tryptophan, positioned about 20-22 amino acids apart ($Wx_{20-22}W$) that function as an interaction module for proline-rich ligands [35]. This domain is also responsible for recruiting Erk1/2 via a polyproline (APPPxxPY) motif [36]. Therefore, we next analyzed the phosphorylation status of Erk1/2 along with the two other MAPKs, Jnk1/2, and p38. All three kinases were active in the WT B cells. p38 phosphorylation was not affected in any of the *Iqgap1*$^{-/-}$ B cells. However, the levels of Erk1/2 and Jnk1/2 phosphorylation were considerably reduced in *Iqgap1*$^{-/-}$ B cells (**Figure 8A**).

Preprints (www.preprints.org) | NOT PEER-REVIEWED | Posted: 7 July 2023 doi:10.20944/preprints202307.0442.v1

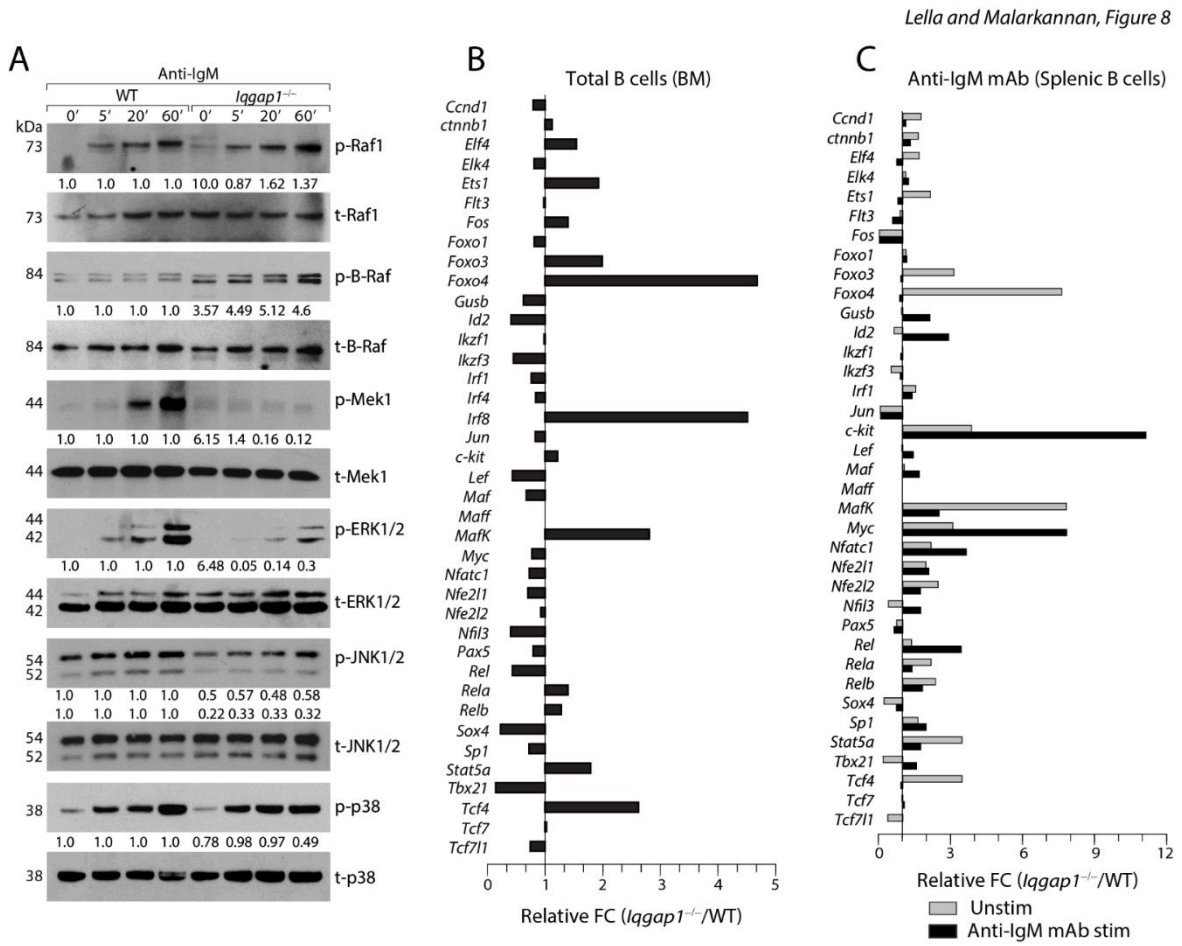

Figure 8. IQGAP1 orchestrates ERK1/2 activation in B cells. A) Sorted splenic B cells were activated with soluble anti-IgM antibody for indicated time points and lysed, protein quantities were estimated and analyzed by western blots. Lysates were analyzed for the total and phosphorylated forms of Raf1, B-Raf, Mek1, Erk1/2, JNK1/2, and p38. Numbers below each blot represent fold change calculated following normalized values against their respective total and based on the phosphorylated protein levels of the WT. **B**) PCR array results. **C**) PCR array results. Data shown are one representative panel of three independent experiments. Data shown are obtained by repeated probing of the same membrane for indicated proteins.

To further define the status of specific transcription factors altered in the early B cells from *Iqgap1*$^{-/-}$ mice, we performed a PCR array analysis. We sorted total B cells from the BM or spleen of three mice each and pooled the mRNA for each strain. cDNA preparations were analyzed in triplicates, and average expression was presented as fold change (Fc) between *Iqgap1*$^{-/-}$ B cells over WT (**Figure 8B**). Total naïve BM B cells were analyzed for the expression levels of transcription factors that play an essential role in early B cell commitment and maturation. Expressions of *Foxo3*, *Foxo4*, *MafK*, *Stat5a*, and *Tcf4* were increased two-fold in *Iqgap1*$^{-/-}$ B cells compared to WT. *Id2*, *Ikzf3*, *Lef*, *Nfil3*, *Rel*, *Sox4*, and *Tbx21* were reduced in the *Iqgap1*$^{-/-}$ B cells. It is important to note that the expression of *Id2* is regulated by Erk/Jnk/Cdk2 pathway. *Ikzf3* (Ailos) is essential for the heterochromatic sequestration of the Igκ gene. Next, we stimulated the sorted splenic B cells with anti-IgM mAb and compared the expression of transcription factors in between unstimulated and stimulated conditions from both strains. Averages from triplicates were used to calculate the fold change (Fc) between *Iqgap1*$^{-/-}$ B cells over WT under both the experimental conditions (**Figure 8C**). Similar to the total B cells from the BM, the levels of *Foxo3*, *Foxo4*, *MafK*, *Stat5a*, and *Tcf4* have increased two or more folds in non-stimulated *Iqgap1*$^{-/-}$ B cells compared to WT. The expression levels of all these factors were considerably reduced in *Iqgap1*$^{-/-}$ B cells following anti-IgM mAb-mediated activation. However, the levels of *c-Fos*, *Jun*, *Sox4*, and *Tbx21* were reduced in both unstimulated and

 doi:10.20944/preprints202307.0442.v1

stimulated conditions. Interestingly, levels of *Id2*, *c-Kit*, *Myc*, *Nfatc1*, and *Rel* were increased in *Iqgap1*$^{-/-}$ B cells following anti-IgM mAb-mediated activation (**Figure 8C**). Expression of c-Kit is limited only to the pre-lymphoid progenitors, pro-B, and pre-B-I cells. Therefore, a high level of c-Kit expression in *Iqgap1*$^{-/-}$ B cells at both unstimulated and stimulated conditions strongly validates our phenotypic characterization and supports our notion that lack of IQGAP1 results in a defect in the transition of pre-B-I into large pre-B-II cells.

IQGAP1 is essential for suppressing Stat5a and Stat5b

Earlier studies have shown that pre-BCR-mediated activation counters the IL-7R pathway [25]. Signaling via IL-7R sustains the survival and proliferation of pro-B cells [37]. This is primarily mediated by cell-cycle-related genes, including *Ccnd3*. In addition, phosphorylated Stat5A and Stat5B, downstream of IL-7R, translocated into the nucleus and form a complex with PRC2/EZH2 to bind to 5′ intronic enhancer of the κ gene (*iE*κ) to actively suppress its transcription by limiting the access to E2A, which is induced by the pre-BCR signaling. In addition, the pre-BCR-mediated Ras-Mek1/2-Erk1/2 pathway silences *Ccnd3* to orchestrate the exit from the cell cycle and to initiate κ chain recombination [25, 38]. First, we investigated the status of *Ccnd3* transcripts. For this, we purified the relatively immature T1 B cells from the spleens of WT and *Iqgap1*$^{-/-}$ mice. Expression of cell cycle-related genes such as β-*catenin*, *Bcl-xl*, *Ccnd3*, *Ccnd1*, and *Bim* were analyzed. We found that the levels of β-*catenin* and *Ccnd3* transcripts were significantly and moderately reduced, respectively (**Supplementary Figure S3**). Next, we investigated the status of E2A, Ezh2, Stat3, Stat5A, and Stat5B in WT and *Iqgap1*$^{-/-}$ B cells. First, we analyzed the protein levels of these transcription factors in the total B cells derived from the BM of both strains (**Figure 9A**). The limited numbers of pro-and pre-B cells excluded our ability to use them in these assays. Compared to the WT, *Iqgap1*$^{-/-}$ B cells possessed moderately higher levels of E2A, Stat5A, Stat5B, and Ezh2.

Preprints (www.preprints.org) | NOT PEER-REVIEWED | Posted: 7 July 2023 doi:10.20944/preprints202307.0442.v1

Lella and Malarkannan, Figure 9

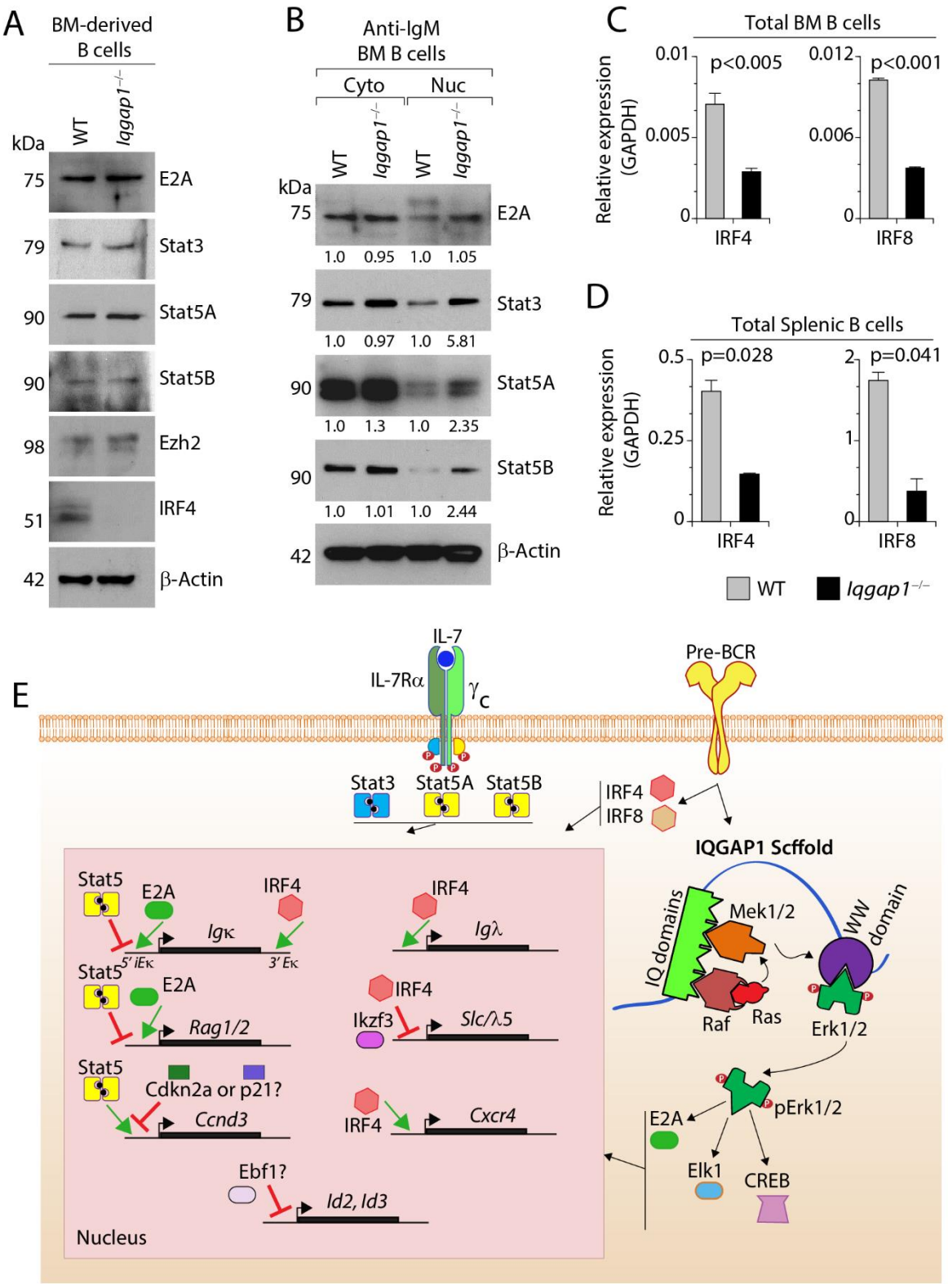

Figure 9. IQGAP1 is required to suppress Stat5a and Stat5b and to initiate the transcription of IRF4 and IRF8. A) Total sorted BM B cells were used to analyze the protein levels of E2A, Stat3, Stat5A, Stat5B, IRF4, and β-actin. Data shown are one representative of three experiments. **B**) Total sorted BM B cells were activated with anti-IgM mAb, and the cytoplasmic and nuclear protein fractions were separated and analyzed for E2A, Stat3, Stat5A, Stat5B, and β-actin. Data shown are one representative of three experiments. **C**) mRNA from sorted BM B cells was used to quantify the expression of *Irf4*

Preprints (www.preprints.org) | NOT PEER-REVIEWED | Posted: 7 July 2023 doi:10.20944/preprints202307.0442.v1

and *Irf8* transcripts. Data shown are the average relative expression of these transcripts from four mice. **D**) mRNA from sorted splenic B cells was used to quantify the expression of *Irf4* and *Irf8* transcripts. Data shown are the average relative expression of these transcripts from four mice. Statistical significance was calculated using Student's *t*-test, and p-values are shown below each graph. **E**) Cartoon summarizing the role of IQGAP1 during early B cell development. IL-7R transduces its signal via Stat3, Stat5A, and Stat5B. Signals via pre-BCR initiate two distinct pathways, One via SLP65-mediated IRF4 and IRF8 activation and the second via the Ras-Raf-Mek-Erk/Jnk pathway mediated by IQGAP1. Four tandemly organized IQ domains can recruit C-Raf or B-Raf. IQ domains also have the specificity to Mek1/2. Rafs mediate the activation of Mek1/2 on the IQGAP1 scaffold. The WW domain of IQGAP1 recruits Erk1/2, which is phosphorylated by Mek1/2. Phosphorylated Erk1/2 activates several transcription factors, including E2A, Elk1, and CREB. E2A competes with Stat5 dimers for the 5′ intronic Eκ enhancer accessibility. Successful displacement of Stat5 dimers initiates the recombination process of Igκ gene. E2A also relieves the Stat5-mediated repression of *Rag1* and *Rag2* genes. Stat5-mediated transcription of Ccnd3 is relieved by the phosphorylated Ras-Mek1/2-Erk1/2 pathway. The potential candidates that repress the transcription of *Ccnd3* are Cdkn2a or p21. The mechanism by which IQGAP1 regulates the expression of *Irf4* and *Irf8* genes are not known. IRF4 binds to the 3′ Eκ in further promoting light chain recombination. IRF4 also binds to the 5′ Eλ to initiate the transcription of Igλ gene. IRF4, along with Ikaros3 (Ailos) represses the surrogate light chain component λ5-encoding gene. IRF4 also plays an important role in initiating the transcription of Cxcr4, which is essential for the pre-B cells to traffic from their IL-7-producing stromal niche to IL-7-deficient niche to transition into immature B cells. Repressing Id2 and Id3 is also needed for the pre-B cells that is regulated by Ebf1, a potential target downstream of Erk1/2.

Interestingly, no protein band was found for IRF4 in *Iqgap1*$^{-/-}$ B cells (**Figure 9A**). Next, we evaluated the levels of these transcription factors translocated into the nucleus following anti-IgM mAb-mediated activation. The B cells activated by this method are not pro- or pre-B cells; but immature and mature B cells. However, it served as an indicator of the status of these transcription factors. We isolated total BM B cells and activated them with anti-IgM mAb for two hours. Nuclear and cytoplasmic fractions were isolated and analyzed for total E2A, Stat3, Stat5A, Stat5B, and β-actin (**Figure 9B**). Stat3, Stat5A, and Stat5B were present at comparable levels in the cytoplasmic fractions of B cells in both the WT and *Iqgap1*$^{-/-}$ mice. However, following anti-IgM mAb-mediated activation, the levels of these transcription factors were higher in *Iqgap1*$^{-/-}$ B cells compared to that of the WT. These results indicate a sustained presence of E2A, Stat3, Stat5A, and Stat5B in the nucleus of *Iqgap1*$^{-/-}$ B cells. In addition to these transcription factors, IRF4 and IRF8 are obligatory for the cycling pre-B to initiate light chain rearrangement and transition into immature B cells [39, 40]. Therefore, next, we quantified the levels of IRF4 and IRF8 in total BM- and spleen-derived B cells. Both IRF4 and IRF8 were significantly reduced in B cells from *Iqgap1*$^{-/-}$ compared to the WT mice (**Figure 9C, D**). These results demonstrate that the lack of IQGAP1 scaffold significantly impairs early B cell development due to the reduced levels of IRF4 and IRF8 transcription factors.

Discussion

In this report, we define that IQGAP1 functions as an essential scaffold regulating the early development and maturation of B cells. Earlier studies have shown that the MAPK/Erk1/2 pathway plays a vital role in most B cell developmental stages and functions [25, 37, 38, 41]. However, the identity of the scaffold proteins and their stage-specific roles were not defined. We found lack of IQGAP1 significantly blocked the transition of pre-B-I cells into large pre-B-II cells in the BM. In conjunction with this blockade, recombination of Igκ and the expression of Igλ chains were moderately reduced.

Furthermore, the lack of IQGAP1 resulted in a significant reduction in the transcription of IRF4 and IRF8, two essential transcription factors for light chain recombination. In the periphery, the splenic NF B and follicular FO B cell numbers were increased, while the MZ B cell numbers were significantly reduced in the *Iqgap1*$^{-/-}$ mice. Our findings demonstrate that these developmental defects are B cell-intrinsic. In addition, the lack of IQGAP1 significantly reduced TD and TI humoral

responses. Mechanistically, the lack of IQGAP1 resulted in the reduction of Mek1/2, Erk1/2, and Jnk1/2 phosphorylation, suggesting a basis for the impaired B cell development and function.

Pre-BCR signaling initiated two major activation pathways. First, one involves the Ras-Raf-Mek-Erk/Jnk pathway. The second pathway involves the PLC-γ2/SLP65/Btk/IRF4/IRF8 signaling. These two pathways are obligatory and converge to attenuate the survival and proliferation signaling regulated by the IL-7R in pro-pre B cells. Earlier studies have shown that the absence of both Erk1 and Erk2 in murine pro-B cells resulted in defective pre-BCR signaling, proliferation, and their transition into pre-B cells [38]. Thus, if the IQGAP1 is an obligatory scaffold for organizing the Ras-Raf-Mek-Erk1/2 pathway, it should impair the proliferation of pro-B cells and their transition into pre-B cells. Although a primitive GTPase-activation-related domain (GRD) is present in IQGAP1 between 1004-1237 amino acids, it lacks GTPase-activating protein (GAP) activity. It thereby is unable to regulate Ras-GTP [42] or Rap-GTP hydrolysis [43]. The crystal structure of the GRD domain demonstrates the presence of a conserved threonine in place of the catalytic 'arginine finger' essential for GTP hydrolysis [44]. Irrespective of lacking a GAP function, IQGAP1 possesses six highly conserved domains, with which it recruits and sequentially activates B-Raf [15, 32, 45], Mek1/2 [30], and Erk1/2 [12, 30, 36, 46]. These earlier findings strongly suggest that IQGAP1 can function as an essential scaffold in developing B cells.

Receptor-mediated stimulations result in Vav1-Cdc42-Pak1 activation, and Pak1 binds to Rafs to induce conformational changes and phosphorylate serine^{445} of B-Raf or serine^{338} of C-Raf [47, 48]. IQGAP1, via its Ras-GAP C-terminus (RGCT) domain (1276-1657 amino acids), recruits the Cdc42-GTP [49] and activates Pak1. Ras is an essential GTPase for the activation of Rafs [50, 51]. B-Raf and C-Raf possess an N-terminal Ras-binding domain (RBD), a ubiquitin-like fold, which functions as an auto-inhibitory domain. Upon Ras-GTPase binding, Rafs are activated to phosphorylate downstream substrates such as Mek1/2. Four tandem Isoleucine-Glutamine (IQ) domains located between 745-864 amino acids contain repeats that are 25 amino acids long and have [I/V/L]Qxxx[RG]xxx[RK] motif, which primarily interacts with Rap1 [31], B-Raf or C-Raf [32], Mek1/2 [30]. Two highly conserved tryptophan within the WW domain (685-710 amino acids) positioned about 20-22 amino acids apart (Wx$_{20\text{-}22}$W) function as an interaction module for proline-rich ligands [35]. This WW domain is responsible for recruiting Erk1/2 via a polyproline (APPPxxPY) motif [36]. Thus, IQGAP1 can orchestrate the Ras→Raf→Mek→Erk pathway in B cells.

We found that the overall absolute number of B cells in terms of B220^{+} (both B220^{High} and B220^{Low} B cells) were significantly increased in the BM of *Iqgap1*$^{-/-}$ mice compared to the WT. Early B cell development in BM is characterized by the expression of CD43 (Leukosialin), CD117 (c-Kit), and CD25 (IL-2Rα). B220^{+}CD43^{+} Pro-B cells develop into B220^{+}CD43^{-} pre-B cells. The absolute cell numbers of Pro-B cells did not differ between *Iqgap1*$^{-/-}$ and WT. However, B220^{Med}CD43^{-} B cells were much higher in *Iqgap1*$^{-/-}$, which is consistent with the increased B220^{+}IgM^{-} pro/pre-B cells populations. Maturing pro-pre-B cells decrease the expression of c-kit and increase the level of CD25. Therefore, we used CD25 (IL-2Rα) as a marker to specify large pre-B (stage-II, early pre-B) and small pre-B (stage-II, late pre-B). Pro-pre-B and pre-B stage-I cells do not express CD25. Immature and mature B cells stop expressing CD25. We found a significant increase in the numbers of B220^{+}CD25^{+} B cells in the BM of *Iqgap1*$^{-/-}$ mice. These findings are validated independently with a PCR array analysis. We found significantly increased levels of c-Kit expression in *Iqgap1*$^{-/-}$ total splenic B cells at both unstimulated and anti-IgM mAb-stimulated conditions. These results demonstrate that lack of IQGAP1 results in a blockade in the transition of pre-B-I into large pre-B-II cells.

As expected, with the increase in the B220^{+}CD43^{+} pro-B cells or B220^{+}CD25^{+} large/small pre-B cells, the B220^{+}IgM^{-} B cells also significantly increased. Notably, the B220^{+}IgM^{+}IgD^{-} immature B cells but not the B220^{+}IgM^{+}IgD^{+} or B220^{+}IgM^{-}IgD^{+} mature B cells were increased in the *Iqgap1*$^{-/-}$ mice. Thus, our data from the BM of non-challenged WT and *Iqgap1*$^{-/-}$ mice imply that IQGAP1 is essential during the early developmental stages of B cells; however, its absence does not negatively impact the commitment to B cell lineage. The light chain rearrangement is moderately but significantly reduced in *Iqgap1*$^{-/-}$ B cells. This may be because other MAPK scaffolds, such as KSR1, may compensate for the absence of IQGAP1. The early developmental progression of B cells is regulated by multiple

Preprints (www.preprints.org) | NOT PEER-REVIEWED | Posted: 7 July 2023 doi:10.20944/preprints202307.0442.v1

soluble factors, including Flt3 ligand, SCF, and IL-7, produced by BM stromal cells. We performed BM chimera experiments to distinguish between the B cell-intrinsic and extrinsic effects. Our findings strongly indicate that the impairments we see in B cells are due to the lack of IQGAP1 within the B cells and the minimal role of cell-extrinsic factors.

BM B cells continue to mature in the spleen [52, 53]. Total $B220^+$ B cells were considerably higher in mice lacking IQGAP1 than the WT, irrespective of comparable numbers of total lymphocytes in both strains. Classification of immature and mature B cells based on their IgM and IgD expression did not show any changes in cell numbers due to the lack of IQGAP1. However, identification of T1, T2, and T3 splenic B cells [53] based on their expression of CD220, CD93 (AA4), IgM, and CD23 revealed a significant increase in the absolute numbers of T1 ($CD220^+CD93^+IgM^+$) B cells. $IgM^{high}IgD^-CD21^-CD23^-$ T1 B cells in the spleen are the continuation of IgM^+ immature B cells in the BM. The lack of IQGAP1 did not alter the numbers of T2 and T3 B cells. One possibility for the higher number of T1 B cells may be due to an impairment in deleting autoreactive B cells in the spleen during their maturation process. The mature T2 and T3 B cells can be further classified into NF B ($B220^+CD21^{Low}CD23^{Low}$), FO B ($B220^+CD21^{Low}CD23^{High}$), and MZ B ($B220^+CD21^{High}CD23^{Low}$) cells. Lack of IQGAP1 moderately increased the numbers of NF B and FO B cells and significantly reduced the numbers of MZ B cells. One possibility for the decrease in the MZ B, but not NF B or FO B, could be the requirement of differing levels of tonic BCR signaling in these subsets. These results indicate that the developmental defects of the B cells in BM extend and persist in the periphery.

Challenging mice with TI and TD antigens *in vivo* indicated that lack of IQGAP1 significantly reduced the ability of B cells to respond and generate IgM, IgG1, IgG2a, IgG2b, and IgG3 antibodies. These functional defects could occur due to two reasons. One, an inherent developmental defect might have resulted in the inability of *Iqgap1*$^{-/-}$ B cells to respond. However, it is also possible that a defective Erk1/2/MAPK pathway leads to functional impairments in partially matured B cells in the *Iqgap1*$^{-/-}$ mice.

Differential expression of cell surface IgM and IgD define immature and mature B cells. The pre-B cells at Stage-II level are cytoplasmic IgM-positive; but stop the expression of surrogate light chains (SLC) composed of λ5 and VpreB [54, 55]. Expression of Rag1 and Rag2 at the late pre-B stage-II ($BP\text{-}1^+$ Fraction-D) initiates the rearrangement of Vκ chains [56]. Thus, expression of cell surface IgM marks the transition of late pre-B into mature B cells. The unique recombining sequence (RS) is a marker of ongoing light chain rearrangement, and it occurs at the time of late κ recombination [29]. Most RS rearrangements occurred in small pre-B cells that possess cytoplasmic $Igμ^+$; but do not express surrogate light chains. At this stage, the pre-B cells start expressing *Rag1* and *Rag2* genes, which are essential for the κ or λ rearrangement [29]. We find that the lack of IQGAP1 resulted in both a reduced RS occurrence and a significantly reduced Igκ and Igλ chains in the sera. Earlier studies have shown that the Ras-mediated MEK-Erk1/2 pathway is crucial for the exit from sustained IL-7-driven cell division and the initiation of light-chain recombination [25, 37]. Our analyses demonstrated that the phosphorylated Mek1, Erk1/2, and Jnk1/2 were considerably reduced in the *Iqgap1*$^{-/-}$ B cells. However, we did not observe any reductions in phosphorylated Raf1 or B-Raf levels. We do not know the precise reasons for these observations. Earlier studies have predicted the hierarchical interplay between IQGAP1 and caveolin scaffolds; however, whether such a mechanism operates in lymphocytes is unknown [51].

The phenotypic and functional outcome of *Iqgap1*$^{-/-}$ B cells provides a model (**Figure 9E**) that concurs with earlier observations. Erk1/2-mediated activation of E2A plays an essential in relieving the Stat5-mediated suppression of Igκ chain recombination [25]. The levels of E2A under unstimulated and anti-IgM mAb-activation did not change in the BM-derived B cells from the WT. Albeit still lower than the WT, its level was increased only after anti-IgM mAb-stimulation in B cells from the BM of *Iqgap1*$^{-/-}$ mice. This demonstrates that under homeostatic conditions, the level of E2A was significantly lower in the BM-derived B cells of *Iqgap1*$^{-/-}$ mice. In addition, our data indicate an increase in the levels of nuclear Stat3, Stat5A, and Stat5B in the BM-derived B cells from *Iqgap1*$^{-/-}$ mice. Thus, a significant increase in the pre-B-I cells and immature B cells could be due to the disruption of Erk1/2 activation and persistence of Stat5 functions. These findings imply that the loss of IQGAP1

Preprints (www.preprints.org) | NOT PEER-REVIEWED | Posted: 7 July 2023 doi:10.20944/preprints202307.0442.v1

leads to a failure to suppress cell-cycle-regulated genes, and this could be due to impaired activation of the ERK pathway by the pre-BCR. Importantly, levels of c-Fos and c-Jun, two crucial AP1 transcription factors regulated by Erk1/2 and Jnk1/2, respectively, were decreased in the *Iqgap1*$^{-/-}$ splenic B cells. Through a second pathway, activation via pre-BCR elevates the transcription of *Irf4* and *Irf8* [40]. This study showed that IRF4 bound to the 3′Eκ and 3′Eλ enhancers and positioned the alleles away from the pericentric chromatin. This, along with the attenuation of the IL-7R-mediated signaling, is required to displace Stat5, followed by the binding of E2A for the activation of iEκ enhancer. Our data indicate a significant reduction in both *Irf4* and *Irf8* transcripts in the BM and splenic B cells derived from *Iqgap1*$^{-/-}$ mice. The reductions in *Irf4* and *Irf8* transcripts are substantial and striking; however, currently, we do not know where and how IQGAP1 links and coordinates the pre-BCR-mediated SLP65 activation. Furthermore, no direct association between SLP65 and IQGAP1 is known. Future studies should focus in defining these molecular interactions.

In summary, we define IQGAP1 as an essential scaffold protein for the development and functions of B cells. IQGAP1 regulates the Ras/Raf→Mek1/2→Erk1/2/Jnk1/2 pathway in pre-B cells, leading to the exit from IL-7R/Stat5-dependent cell cycle and the entry into Igκ light chain recombination. In addition, through an unknown mechanism, IQGAP1 is involved in initiating the transcription of IRF4 and IRF8 that are required for the transition of pre-B into immature B cells. Lack of IQGAP1 significantly reduced the humoral responses against both TD and TI B cell responses. Future studies should focus on further delineating the molecular mechanisms regulated by IQGAP1 and other scaffold proteins.

Materials and Methods

Mice

Iqgap1$^{-/-}$ mice in the C57BL/6 background [20] were used along with the C57BL/6 (WT, Jackson Laboratory, Bar Harbor, Maine) as controls. Mice used for this study were maintained in the Biology Resource Center (BRC) at the Medical College of Wisconsin (MCW) in their pathogen-free facility and were used for experiments between the ages of 6 and 12 weeks of age. All animal protocols were approved by Institutional Animal Care and Use Committees of the IACUC at the Medical College of Wisconsin, Milwaukee, WI. In addition, medical College of Wisconsin is formally accredited by AAALAC, and all the animal care and use-protocols used in this study fully adhere to the specified guidelines of AAALAC.

Flow cytometry

Single-cell suspensions were prepared by gently mincing the dissected organs through 70-μm cell strainers. Single-cell preparations were stained with fluorescent-labeled mAbs in a FACS buffer (PBS containing 5% BSA and 0.5% Sodium Azide solution) for half an hour and washed with the FACS buffer twice. Flow cytometry analyses were conducted in LSR-II (BD Biosciences, San Jose, CA) or MACSQuant Analyzer 10 (Miltenyi Biotec, Bergisch Gladbach, Germany) and analyzed with FlowJo software (FlowJo LLC, Ashland, OR). We used the following antibodies purchased from eBioscience at Thermo-Fischer (Waltham, MA) for flow cytometry: rat anti-mouse B220 (RA3-6B2), rat anti-mouse IgM (R6-60.2), rat anti-mouse IgD (11-26c.2a), rat anti-mouse CD19 (1D3), rat anti-mouse CD1d (1B1), rat anti-mouse CD21/CD35 (4E3), rat-anti-mouse CD23 (B3B4), Armenian hamster anti-moue CD3ε (145-2C11), rat anti-mouse CD16/CD32(93), rat anti-mouse CD43, rat anti-mouse CD23 (B3B4), rat anti-mouse CD93 (AA4.1), rat anti-mouse CD25 and IL-4 (eBioscience, San Diego, CA); rat anti-mouse c-Kit (BD Pharmingen, San Jose, CA); MOMA-1-FITC (Serotec, Raleigh, NC); goat anti-mouse IgM F(ab′)2 (Jackson ImmunoResearch, West Grove, PA, USA); mouse anti-b-actin. For analyzing NF, FO, and MZ B cell populations, single-cell suspensions from spleens were stained with anti-B220-Pacific Blue, anti-CD21-FITC, and anti-CD23-PE-Cy7 mAbs and sorted using FACSAria (BD Biosciences, San Jose, CA). Splenic T1, T2, and T3 cells were characterized by gating for B220^{+}CD93^{+} B cells and analyzing with IgM/CD23 positivity.

 doi:10.20944/preprints202307.0442.v1

B cell separation and cell sorting

Resting B cells were purified using B cell isolation kit (Miltenyi Biotech Inc., Auburn CA). Total B cells were also sorted using markers including B220 and CD19. T1 B cells, Follicular B or Marginal zone B cells were isolated with gating strategies involving B220/CD93/IgM/CD23, B220/CD21/CD23 panels as indicated in the results section. Separated cells were stained with anti-CD19 and anti-CD3ε mAbs, and their purity was more than 95%, as confirmed by flow cytometry. Viability of the sorted cells were tested using trphan blue stain exclusion.

Clonotyping

Isotyping pre or post-immune sera and quantifying k or l chains in the sera were done using SBA Clonotyping System-HRP kit, a sandwich ELISA-based assay (SouthernBiotech, Birmingham, AL, USA).

Immunohistochemistry staining

Spleens were embedded in Tissue-Tek (Sakura Finetek, Zoeterwoude, The Netherlands), frozen with the dry-ice-Isopropanol mixture, and kept at -80°C until sectioning. 10 μm cryostat sections were generated, air-dried for 1h at room temperature (RT), and fixed in acetone for 10 min. The sections were blocked with 0.1% BSA/PBS containing anti-CD16/CD32 mAb for 45 min, incubated for 1h at RT in the dark with the rat anti-mouse CD3ε-PE, anti-B220-Cy5, MOMA-1-FITC, anti-mouse IgM-PE or anti-mouse IgD-FITC mAbs. Sections were mounted in an aqueous mounting medium and visualized on Olympus FV1000 Two Photon Confocal microscope. Pictures were taken at 40 × magnification.

Bone marrow transplantation (BMT)

BM cells from tibias and femurs of WT and *Iqgap1*$^{-/-}$ mice were prepared and resuspended in 2% FBS/RPMI1640 (Invitrogen Life Technologies, Carlsbad, CA). 5 × 10^6 BM cells (200 μl) were injected intravenously to reconstitute 6-8 weeks old, lethally (1100 rads) irradiated WT or *Iqgap1*$^{-/-}$ mice 4h after the irradiation. The recipient mice were sacrificed 8 weeks later, and the spleens were analyzed for reconstitution of B cells by flow cytometry.

Western blotting

B cells were purified from spleens and resuspended in HEPES buffer (10mM HEPES/0.5% FCS/RPMI 1640). 15×10^6 B cells were used for each lane. Cells were stimulated with 50 μg/ml goat-anti-mouse IgM F(ab')$_2$ for 2 min at 37°C or left unstimulated. Stimulation was terminated by adding one volume of 2× ice-cold lysis buffer (100 mM Tris [pH 7.4], 150 mM NaCl, 2% NP-40, 1% deoxycholic acid, 0.2% SDS, 2 mM sodium orthovanadate, with phosphatase inhibitor cocktail, PhosSTOP (Roche Diagnostics GmbH, Mannheim, Germany) and proteinase inhibitor cocktail (Sigma, St Louis, MO). Lysates were incubated for 30 min on ice, and centrifuged at 15,000*g* for 15 min at 4°C. For Western blotting, cell lysate aliquot (corresponding to 1×10^6 cells) were separated by SDS-PAGE, transferred to PVDF membrane, and probed with primary and secondary Abs conjugated with horseradish peroxidase. The membranes were probed with the indicated antibody, and the signal was detected using either SuperSignal West Pico Chemiluminescent substrate or Dura (Thermo Scientific, Waltham, MA). We used the following antibodies: phospho-C-Raf (Ser338) (MilliporeSigma, Burlington MA), ⊚-Actin (ACTBD11b7) (Santa Cruz, Dallas, TX). We also used the following antibodies from Cell Signaling Technology (Danvers, MA): phospho-MEK1/2(Ser221, 166F8), MEK1/2 (47E6), phosphor-Erk1/2 (Thr202/Tyr204, D13.14.4E) , Erk1/2 (137F5), phosphor-Jnk1/2 (Thr183/Tyr185, 98F2) , Jnk1/2 (9252) phospho-p38 (Thr180/Tyr182, 3D7), p38, phospho-B-Raf (Ser445), anti-E2A (D2B1), anti-Stat3 (124H6), anti-Stat5A (4H1), anti-Stat5B (34662), anti-Ezh2 (D2C9), anti-IRF4 (15106). The fold change in phosphorylation following 5, 20, or 60 min of activation was calculated using this normalized value by comparing it with that value in the unstimulated lane

 doi:10.20944/preprints202307.0442.v1

(normalized phospho-protein value after 5/20/60 min of activation/normalized phospho-protein value in the unstimulated lane).

T-dependent and T-independent humoral responses

For TI immune response, 6-8 weeks-old mice were immunized intraperitoneally with 100 μg of TNP-Ficoll (Biosearch Technology, Novato, CA) in PBS. 50 μl of blood was collected from the retro-orbital venous plexus with capillary tubes on days 0 and 7 after immunization. For TD response, mice were intraperitoneally injected with 100 μg TNP-KLH in 200 μl of aluminum hydroxide adjuvant, Imject Alum (Pierce, Rockford, IL) and boosted with10 μg of TNP-KLH without adjuvant on day 21. Sera were collected on days 0, 7, and 28. Sera were analyzed by ELISA for basal and TNP-specific immunoglobulin isotypes using SBA Clonotyping system (SouthernBiotech, Birmingham, AL).

Heavy (CDR3) and Light chain (Vκ-RS) chain rearrangements

Semiquantitative PCR with genomic DNA was done as previously described [29, 40]. The following primers were used to define the heavy chain rearrangements. Degenerate V_κ and *Igk* intron primers and five-fold template dilutions were used for PCR. Spectrotyping (Fragment analysis) following DNA sequencing (3500 Genetic Analyzer, Applied Biosystems) was done using Peak Scanner Software. Electropherogram records of amplified fragments were collected and analyzed. JH region (5′-CTTACCTGAGGAGACGGTGA-3′; Forward primers were the following: MIGHV1, 5′-TCCAGCACAGCCTACATGCAGCTC-3′; MIGHV2, 5′-CAGGTGCAGCTGAAGGAGTCAGG-3′; MIGHV3, 5′-AGGTGCAGCTTCAGGAGTCAGG-3′; MIGHV5, 5′-CAGCTGGTGGAGTCTGGGGGA-3′; MIGHV6, 5′-AAGTGAAGCTTGAGGAGTCTGG-3′; and MIGHV7, 5′-AGGTGAAGCTGGTGGAGTCTGG-3′. The following primers were used to define the light chain rearrangements. Forward primer: 5′-AGCTTCAGTGGCAGTGGRTCWGGRAC-3′; Reverse primer: 5′-ACATGGAAGTTTTCCTGGGAGAATATG-3′

PCR Array analyses

We performed the RT-qPCR using custom-made amplicons for the indicated genes [57]. Assays were done using BioMark™ Real-Time PCR System and the Digital Array Chip from Fluidigm Inc (San Francisco, CA, USA) as described earlier [58]. This multiplexed digital array uses a microfluidic dynamic array platform in conjunction with multiplexed RT reactions for mRNA profiling. cDNAs were diluted 1:5 with ddH_2O, and the assay was performed in a 48×48 dynamic array. Briefly, a 5 μl sample mixture was prepared for each sample containing 1 × TaqMan Universal Master Mix (No UNG), 1 × GE Sample Loading Reagent (Fluidigm PN 85000746) and each of diluted pre-amplified cDNA. 5 μl of Assay mix was prepared with 1 × each of TaqMan miRNA assay and 1 × Assay Loading Reagent (Fluidigm PN 85000736). An IFC controller was used to prime the fluidics array (chip) with control line fluid and then with samples and assay mixes in the appropriate inlets. After loading, the chip was placed in the BioMark for PCR at 95°C for 10 min, followed by 40 cycles at 95°C for 15 sec and 60°C for 1 min. Five house-keeping genes (*beta-glucuronidase*, Mm.3317; *Hprt*, Mm.299381; *Hsp70ab1*, Mm.2180; *GAPDH*, Mm.343110;, *and beta-actin*, Mm.328431) were used to normalize the data. Mouse genomic DNA, positive PCR controls, and RT controls were used as suggested by Fluidgm Inc. The data was analyzed with Real-Time PCR Analysis Software in the BioMark instrument (Fluidigm Inc, San Francisco, CA, USA).

RT-qPCR

For *Irf4*, *Irf4*, *b-catenin*, *Bcl-xL*, *Ccnd3*, *Ccnd1*, and *Bim* mRNA quantification, sorted BM or splenic B cells from WT and *Iqgap1*$^{-/-}$ mice were processed for RNA extraction (RNeasy Mini Kit; QIAGEN). Next, cDNA was generated using the iScript cDNA synthesis kit (Bio-Rad Laboratories) according to the manufacturer's instructions. Real-time PCR was performed by using a previously published SYBR green protocol with an ABI7900 HT thermal cycler [59]. Transcript in each sample was assayed in triplicate, and the mean cycle threshold was used to calculate the x-fold change and control changes

 doi:10.20944/preprints202307.0442.v1

for each gene using ΔΔCt. Each experiment used the control (housekeeping) gene actb for global normalization.

Graphs

DeltaGraph 5 (Red Rock Software Inc, Salt Lake City, UT) or PRISM GraphPad 9.0 (San Diego, CA) were used for statistical analysis of data and generation of figure graphs

Statistical methods

Number of animals used to generate each panel are shown within the figures or main text. Data presented in each figure were from a minimum of three independent experiments. Raw data were analyzed with the unpaired Student's *t*-test and analysis of variance, followed by the least-significant difference test for comparisons within or between groups. Significant *P* values (<0.05) are presented in each one of the figures.

Supplementary Materials: The following supporting information can be downloaded at the website of this paper posted on Preprints.org. Supplementary Figure S1. Dysregulated early B cell development in the BM of *Iqgap1*$^{-/-}$ mice is B cell-intrinsic. Indicated host mice were sub-lethally irradiated and reconstituted with donor-derived 5 × 10^5 BM cells. Eight weeks later, cells from the host BM were harvested and analyzed. A, B) Viable cells within the lymphocyte gate were analyzed for the absolute number of total B cells. Staining with anti-B220 antibody indicated the presence of both $B220^{High}$ and $B220^{Low}$ B cells in both the WT and *Iqgap1*$^{-/-}$ mice. Total cell numbers in each subset were enumerated from six reconstituted mice and shown on right-side panels. C) Absolute numbers of reconstituted $B220^+IgM^-$ pro/pre-B, $B220^+IgM^+$ immature B, and $B220^{Hi}$ recirculating B cells were defined using anti-B220 and anti-IgM antibodies, and their numbers were calculated from live lymphocyte gates. Data shown on the left are representative panels. Data shown are from two independent experiments with three mice each. Data are shown with the mean ± SEM. Statistical significance was calculated using Student's *t*-test, and p-values are shown below each graph. Supplementary Figure S2. Impairment in the splenic B cell development in *Iqgap1*$^{-/-}$ mice is cell-intrinsic. Indicated host mice were sub-lethally irradiated and reconstituted with donor-derived 5 × 10^5 BM cells. Eight weeks later, cells from the host spleens were harvested and analyzed. A) Absolute total splenic B cells were comparable between the WT and *Iqgap1*$^{-/-}$ mice. Viable cells within the lymphocyte gate were analyzed for the absolute number of total B cells using an anti-B220 antibody. Data shown represent the $B220^+$ B cells per spleen from both strains. B) Absolute numbers of immature and mature B cells do not differ between the WT and *Iqgap1*$^{-/-}$ mice. Total splenic B cells were stained with anti-B220, anti-IgM, and anti-IgD antibodies. Data shown represent the $B220^+IgM^+$ immature B and $B220^+IgM^+IgD^+$ or $B220^+IgM^-IgD^+$ mature B cells. Data represent absolute numbers of immature or mature B cells per spleen from both strains. Data are shown with the mean ± SEM. Statistical significance was calculated using Student's *t*-test, and p-values are shown below each graph. Supplementary Figure S3. Expression levels *Ccnd3* is moderately increased, and β-catenin is significantly decreased in T1 B cells. Total mRNA was isolated from sorted splenic T1 B cells. RTqPCR was performed to quantify the expression levels of *β-catenin*, *Bcl-xl*, *Ccnd3*, *Ccnd1*, and *Bim*. Statistical significance was calculated using Student's *t*-test, and p-values are shown below each graph.

Author Contributions. RKL designed the study and performed experiments, data collection, analysis, and drafted the original manuscript. SM conceived of the study, participated in its design, and performed data analysis and writing of the manuscript. All authors have read and approved the final draft of the manuscript.

Funding. NIH R01 AI102893 (S.M.) and NCI R01 CA179363 (S.M.); Alex Lemonade Stand Foundation (S.M.); HRHM Program of MACC Fund/Children's Hospital of Wisconsin (S.M.), Nicholas Family Foundation (S.M.); Gardetto Family (S.M.); MCW-Cancer Center-Large Seed Grant (S.M.); and Advancing Healthier Wisconsin (S.M.).

Acknowledgments. We thank Dr. Andre Bernards, MGH Cancer Center, Massachusetts General Hospital, MA, for providing the original IQGAP1 knockout mice. We thank Fluidgm corporation for their help with the Digital Array Chip analyses. We also thank the former and current lab members who helped in performing experiments, genotyping mice, and discussions.

Conflicts of Interest. The authors declare that this study was conducted in the absence of any commercial or financial relationships that could be construed as a potential conflict of interest.

Ethics Statement. All mice used in this study were utilized responsibly, and all protocols were approved by the institutional IACUC committee at the Medical College of Wisconsin (MCW), Milwaukee, WI.

References

1. Sacks, D.B. The role of scaffold proteins in MEK/ERK signalling. *Biochem. Soc. Trans* **34**, 833-836 (2006).
2. Ren, J.G., Li, Z. & Sacks, D.B. IQGAP1 modulates activation of B-Raf. *Proc Natl Acad Sci U S A* **104**, 10465-10469 (2007).
3. McNulty, D.E., Li, Z., White, C.D., Sacks, D.B. & Annan, R.S. MAPK scaffold IQGAP1 binds the EGF receptor and modulates its activation. *J Biol. Chem* **286**, 15010-15021 (2011).
4. Sbroggio, M. *et al.* ERK1/2 activation in heart is controlled by melusin, focal adhesion kinase and the scaffold protein IQGAP1. *J Cell Sci* **124**, 3515-3524 (2011).
5. Liu, X.Y. *et al.* IQGAP1/ERK regulates fear memory formation via histone posttranslational modifications induced by HDAC2. *Neurobiol Learn Mem* **171**, 107210 (2020).
6. Briggs, M.W. & Sacks, D.B. IQGAP proteins are integral components of cytoskeletal regulation. *EMBO Rep* **4**, 571-574 (2003).
7. Weissbach, L. *et al.* Identification of a human rasGAP-related protein containing calmodulin-binding motifs. *J. Biol. Chem* **269**, 20517-20521 (1994).
8. Wang, S. *et al.* IQGAP3, a novel effector of Rac1 and Cdc42, regulates neurite outgrowth. *J. Cell Sci* **120**, 567-577 (2007).
9. Schmidt, V.A. *et al.* IQGAP2 functions as a GTP-dependent effector protein in thrombin-induced platelet cytoskeletal reorganization. *Blood* **101**, 3021-3028 (2003).
10. Cupit, L.D., Schmidt, V.A., Miller, F. & Bahou, W.F. Distinct PAR/IQGAP expression patterns during murine development: implications for thrombin-associated cytoskeletal reorganization. *Mamm. Genome* **15**, 618-629 (2004).
11. Brill, S. *et al.* The Ras GTPase-activating-protein-related human protein IQGAP2 harbors a potential actin binding domain and interacts with calmodulin and Rho family GTPases. *Mol. Cell Biol* **16**, 4869-4878 (1996).
12. Nojima, H. *et al.* IQGAP3 regulates cell proliferation through the Ras/ERK signalling cascade. *Nat. Cell Biol* **10**, 971-978 (2008).
13. Abel, A.M. *et al.* IQGAP1: insights into the function of a molecular puppeteer. *Mol Immunol* **65**, 336-349 (2015).
14. Brown, M.D. & Sacks, D.B. Protein scaffolds in MAP kinase signalling. *Cell Signal* **21**, 462-469 (2009).
15. Awasthi, A. *et al.* Rap1b facilitates NK cell functions via IQGAP1-mediated signalosomes. *J Exp Med* **207**, 1923-1938 (2010).
16. Abel, A.M. *et al.* IQ Domain-Containing GTPase-Activating Protein 1 Regulates Cytoskeletal Reorganization and Facilitates NKG2D-Mediated Mechanistic Target of Rapamycin Complex 1 Activation and Cytokine Gene Translation in Natural Killer Cells. *Front Immunol* **9**, 1168 (2018).
17. Wang, J.C. *et al.* The Rap1-cofilin-1 pathway coordinates actin reorganization and MTOC polarization at the B cell immune synapse. *J Cell Sci* **130**, 1094-1109 (2017).
18. Fukata, M. *et al.* Regulation of cross-linking of actin filament by IQGAP1, a target for Cdc42. *J Biol Chem* **272**, 29579-29583 (1997).
19. Tanos, B.E., Yeaman, C. & Rodriguez-Boulan, E. An emerging role for IQGAP1 in tight junction control. *Small GTPases* **9**, 375-383 (2018).
20. Li, S., Wang, Q., Chakladar, A., Bronson, R.T. & Bernards, A. Gastric hyperplasia in mice lacking the putative Cdc42 effector IQGAP1. *Mol Cell Biol* **20**, 697-701 (2000).
21. Gorman JA, G.T., Billadeau DA. IQGAP1 mediates lymphocyte cytoskeletal polarization and peripheral effector functions. *The Journal of Immunology* **182** (2009).
22. Pillai, S., Cariappa, A. & Moran, S.T. Marginal zone B cells. *Annu. Rev. Immunol* **23**, 161-196 (2005).
23. Carey, J.B., Moffatt-Blue, C.S., Watson, L.C., Gavin, A.L. & Feeney, A.J. Repertoire-based selection into the marginal zone compartment during B cell development. *J Exp Med* **205**, 2043-2052 (2008).
24. Novobrantseva, T.I. *et al.* Rearrangement and expression of immunoglobulin light chain genes can precede heavy chain expression during normal B cell development in mice. *J Exp Med* **189**, 75-88 (1999).
25. Mandal, M. *et al.* Ras orchestrates exit from the cell cycle and light-chain recombination during early B cell development. *Nat. Immunol* **10**, 1110-1117 (2009).
26. Khan, S.N. *et al.* Editing and escape from editing in anti-DNA B cells. *Proc Natl Acad Sci U S A* **105**, 3861-3866 (2008).
27. Luning Prak, E.T., Monestier, M. & Eisenberg, R.A. B cell receptor editing in tolerance and autoimmunity. *Ann N Y Acad Sci* **1217**, 96-121 (2011).
28. Walter, J.E. *et al.* Expansion of immunoglobulin-secreting cells and defects in B cell tolerance in Rag-dependent immunodeficiency. *J Exp Med* **207**, 1541-1554 (2010).
29. Panigrahi, A.K. *et al.* RS rearrangement frequency as a marker of receptor editing in lupus and type 1 diabetes. *J Exp Med* **205**, 2985-2994 (2008).

30. Roy, M., Li, Z. & Sacks, D.B. IQGAP1 is a scaffold for mitogen-activated protein kinase signaling. *Mol Cell Biol* **25**, 7940-7952 (2005).
31. Jeong, H.W., Li, Z., Brown, M.D. & Sacks, D.B. IQGAP1 binds Rap1 and modulates its activity. *J Biol. Chem* **282**, 20752-20762 (2007).
32. Ren, J.G., Li, Z. & Sacks, D.B. IQGAP1 modulates activation of B-Raf. *Proc. Natl. Acad. Sci. U. S. A* **104**, 10465-10469 (2007).
33. Mason, C.S. *et al.* Serine and tyrosine phosphorylations cooperate in Raf-1, but not B-Raf activation. *EMBO J* **18**, 2137-2148 (1999).
34. Yin, X.L., Chen, S., Yan, J., Hu, Y. & Gu, J.X. Identification of interaction between MEK2 and A-Raf-1. *Biochim. Biophys. Acta* **1589**, 71-76 (2002).
35. Macias, M.J., Wiesner, S. & Sudol, M. WW and SH3 domains, two different scaffolds to recognize proline-rich ligands. *FEBS Lett* **513**, 30-37 (2002).
36. Roy, M., Li, Z. & Sacks, D.B. IQGAP1 binds ERK2 and modulates its activity. *J Biol. Chem* **279**, 17329-17337 (2004).
37. Fleming, H.E. & Paige, C.J. Pre-B cell receptor signaling mediates selective response to IL-7 at the pro-B to pre-B cell transition via an ERK/MAP kinase-dependent pathway. *Immunity* **15**, 521-531 (2001).
38. Yasuda, T. *et al.* Erk kinases link pre-B cell receptor signaling to transcriptional events required for early B cell expansion. *Immunity* **28**, 499-508 (2008).
39. Lu, R., Medina, K.L., Lancki, D.W. & Singh, H. IRF-4,8 orchestrate the pre-B-to-B transition in lymphocyte development. *Genes Dev* **17**, 1703-1708 (2003).
40. Johnson, K. *et al.* Regulation of immunoglobulin light-chain recombination by the transcription factor IRF-4 and the attenuation of interleukin-7 signaling. *Immunity* **28**, 335-345 (2008).
41. Rowland, S.L., DePersis, C.L., Torres, R.M. & Pelanda, R. Ras activation of Erk restores impaired tonic BCR signaling and rescues immature B cell differentiation. *J Exp Med* **207**, 607-621 (2010).
42. Morgan, C.J., Hedman, A.C., Li, Z. & Sacks, D.B. Endogenous IQGAP1 and IQGAP3 do not functionally interact with Ras. *Sci Rep* **9**, 11057 (2019).
43. Brown, M.D. & Sacks, D.B. IQGAP1 in cellular signaling: bridging the GAP. *Trends Cell Biol* **16**, 242-249 (2006).
44. Kurella, V.B. *et al.* Crystal structure of the GTPase-activating protein-related domain from IQGAP1. *J. Biol. Chem* **284**, 14857-14865 (2009).
45. Ren, J.G., Li, Z. & Sacks, D.B. IQGAP1 integrates Ca2+/calmodulin and B-Raf signaling. *J. Biol. Chem* **283**, 22972-22982 (2008).
46. Sbroggio, M. *et al.* IQGAP1 regulates ERK1/2 and AKT signalling in the heart and sustains functional remodelling upon pressure overload. *Cardiovasc. Res* **91**, 456-464 (2011).
47. King, A.J., Wireman, R.S., Hamilton, M. & Marshall, M.S. Phosphorylation site specificity of the Pak-mediated regulation of Raf-1 and cooperativity with Src. *FEBS Lett* **497**, 6-14 (2001).
48. Zang, M., Hayne, C. & Luo, Z. Interaction between active Pak1 and Raf-1 is necessary for phosphorylation and activation of Raf-1. *J. Biol. Chem* **277**, 4395-4405 (2002).
49. Joyal, J.L. *et al.* Calmodulin modulates the interaction between IQGAP1 and Cdc42. Identification of IQGAP1 by nanoelectrospray tandem mass spectrometry. *J. Biol. Chem* **272**, 15419-15425 (1997).
50. Marais, R., Light, Y., Paterson, H.F. & Marshall, C.J. Ras recruits Raf-1 to the plasma membrane for activation by tyrosine phosphorylation. *EMBO J* **14**, 3136-3145 (1995).
51. Vetterkind, S., Poythress, R.H., Lin, Q.Q. & Morgan, K.G. Hierarchical scaffolding of an ERK1/2 activation pathway. *Cell Commun. Signal* **11**, 65 (2013).
52. Hardy, R.R. & Hayakawa, K. A developmental switch in B lymphopoiesis. *Proc. Natl. Acad. Sci. U. S. A* **88**, 11550-11554 (1991).
53. Loder, F. *et al.* B cell development in the spleen takes place in discrete steps and is determined by the quality of B cell receptor-derived signals. *J Exp. Med* **190**, 75-89 (1999).
54. Li, Y.S., Hayakawa, K. & Hardy, R.R. The regulated expression of B lineage associated genes during B cell differentiation in bone marrow and fetal liver. *J. Exp. Med* **178**, 951-960 (1993).
55. Shaffer, A.L. & Schlissel, M.S. A truncated heavy chain protein relieves the requirement for surrogate light chains in early B cell development. *J Immunol* **159**, 1265-1275 (1997).
56. van Zelm, M.C. *et al.* Ig gene rearrangement steps are initiated in early human precursor B cell subsets and correlate with specific transcription factor expression. *J Immunol* **175**, 5912-5922 (2005).
57. Spurgeon, S.L., Jones, R.C. & Ramakrishnan, R. High throughput gene expression measurement with real time PCR in a microfluidic dynamic array. *PLoS One* **3**, e1662 (2008).
58. Kolbert, C.P. *et al.* Multi-platform analysis of microRNA expression measurements in RNA from fresh frozen and FFPE tissues. *PLoS One* **8**, e52517 (2013).
59. Yu, S. *et al.* Quantitative real-time polymerase chain reaction for the verification of genomic imbalances detected by microarray-based comparative genomic hybridization. *Genet Test Mol Biomarkers* **13**, 751-760 (2009).